local state feedback is very difficult. The results presented in Section IV shows that one could reduce the stabilization problem to a solvability problem of an algebraic Riccati equation in which the matrix $Q$ may not be nonnegative and there are two "parameter matrices" $W$ and $G$, the choice of which are directly related to the resolution of the stabilization problem.

## REFERENCES


[1] B. T. O'Connor and T. S. Hwang, "Stability of general two-dimensional recursive filters," in *Two-Dimensional Signal Processing I, Linear Filters*, (T. S. Hwang, Ed) Springer-Verlag, 1981.

[2] R. P. Roesser, "A discrete state-space model for linear image processing," *IEEE Automat. Contr.*, vol. AC-20, pp. 1–10, 1975.

[3] S. Y. Kung, B. C. Lévy, M. Morf, and T. Kailath, "New results in 2-D system theory, Part II: 2-D state-space model—Realization and the notions of controllability, observability, and minimality," *Proc. IEEE*, vol. 65, pp. 945–961, 1977.

[4] M. S. Piekarski, "Algebraic characterization of matrices whose multivariable characteristic polynomial is Hurwitzian," in *Proc. Int. Symp. Operator Theory*, (Lubbock, Tx), 121–126, Aug. 1977.

[5] J. H. Lodge and M. M. Fahmy, "Stability and overflow oscillations in 2-D state space digital filters," *IEEE Acoust., Speech, Signal Processing*, ASSP-29, 1161–1171, 1981.

[6] W. S. Lu and E. B. Lee, "Stability analysis for two-dimensional systems," *IEEE Circuits Syst.*, vol. CAS-30, pp. 455–461, July 1983.

[7] D. Goodman, "Some stability properties of two-dimensional linear shift-invariant digital filters," *IEEE Circuits Syst.*, vol. CAS-24, pp. 201–208, 1977.

[8] S. D. Brierly, J. N. Chiasson, E. B. Lee, and S. H. Zak, "On stability independent of delay for linear systems," *IEEE Automat. Contr.*, vol. AC-27, pp. 252–254, 1982.

[9] G. W. Steawart, "Error and perturbation bounds for subspaces associated with certain eigenvalue problems," *SIAM Rev.*, vol. 15, 727–764, 1973.

[10] K. Mårtensson, "On the matrix Riccati equation," *Inform. Sci.*, vol. 3, pp. 17–49, 1971.


**Wu-Sheng Lu** received the equivalent of the B.S. and M.S. degrees, both in mathematics from Fudan University and East China Normal University, Shanghai, China, in 1964 and 1980, respectively, and the M.S.E.E. degree from the University of Minnesota, Minneapolis, in 1983. During the 1983–1984 academic year, he was awarded a Ph.D. dissertation Fellowship by the Graduate School of the University of Minnesota and is currently completing his Ph.D. studies in the Center for Control Science and Dynamical Systems, University of Minnesota.

His recent research interests include multidimensional system theory, optimal control, and the numerical aspects of linear system theory.

**E. Bruce Lee** (M'77–SM'82–F'83) received the B.S. and M.S. degrees in mechanical engineering from the University of North Dakota, Grand Forks, in 1955 and 1956, respectively, and the Ph.D. degree from the University of Minnesota, Minneapolis, in 1960.

From 1956 to 1963 he was employed by Honeywell Inc. to develop digital inertial sensors and control system design techniques. Since 1963 he has been employed by the University of Minnesota, where he is currently Professor of Electrical Engineering and Acting Head of the Electrical Engineering Department.

# Explicit Formulas for Lattice Wave Digital Filters

LAJOS GAZSI, SENIOR MEMBER, IEEE

*Abstract* —**Explicit formulas are derived for designing lattice wave digital filters of the most common filter types, for Butterworth, Chebyshev, inverse Chebyshev, and Cauer parameter (elliptic) filter responses. Using these formulas a direct top down design method is obtained and most of the practical design problems can be solved without special knowledge of filter synthesis methods. Since the formulas are simple enough also in the case of elliptic filters, the design process is sufficiently simple to serve as basis in the first part (filter design from specs to algorithm) of silicon compilers or applied to high level programmable digital signal processors.**

## I. INTRODUCTION

WAVE DIGITAL filters (WDF's) [1] have some notable advantages [2]: excellent stability properties even under nonlinear operating conditions resulting from overflow and roundoff effects, low coefficient wordlength requirements, inherently good dynamic range, etc. All these properties are essentially a consequence of the fact that WDF's, if properly designed, behave completely like passive circuits.

For a proper design the full apparatus of the classical filter synthesis techniques (including those for microwave filters) can be made use of, which guarantees a solid mathematical basis of the WDF's. This fact, however, could be a serious hindrance when the designer is not familiar with the intricate techniques of the classical network theory (e.g., in the case of signal processing applications in medical, seismic, image, speech area etc, where the companies and institutions may not have available for this purpose specialized filter design groups, as well as programming and computer facilities).

Manuscript received May 26, 1983; revised December 8, 1983.

The author is with Ruhr-Universität Bochum, Lehrstuhl für Nachrichtentechnik, D-4630 Bochum 1, West Germany.

0098-4094/85/0100-0068$01.00 

The fact that the papers about various design aspects of WDF's are spread over several journals and sometimes not easily accessible conference proceedings worsens the chance of a faultless outcome of the design.

Therefore, direct methods for designing WDF's, e.g., explicit formulas for element values are of considerable interest, in as far as they are simple or even exist.

It is well known that for WDF's there exists a great number of different structures according to the different realisation possibilities of the reference filters [2]. Fortunately, one can find some algorithms among these structures whose design can be carried out by using explicit formulae and simultaneously these algorithms are general enough to satisfy the most common low-pass, high-pass, bandpass, and bandstop frequency-domain requirements.

In this paper, we will present direct design methods for lattice WDF's [3] where both lattice branches are realized by cascaded first- and second-degree all-pass sections. Other structures where a direct design is possible using explicit formulas will be discussed elsewhere. Furthermore, we will restrict ourselves to the realization of low-pass (high-pass) filters, because by means of network transformations a variety of other filter types such as high-pass, bandpass, and bandstop filters can be very easily derived from a certain low-pass filter.

The purpose of this paper is twofold. In the first part a brief treatment for specialists is given about the construction of the explicit formulas. In the second part we will present for these filters a design procedure which may be used directly without requiring a complete understanding of the underlying methods (we will there omit any proof), thus providing powerful tools for the design engineer.

Now we will first recapitulate briefly some basic definitions of the lattice WDF's. Following these we will prove an important property of the most common lattice WDF's concerning the distribution of their poles among the lattice branches. Then we present explicit formulae for designing the most common, i.e., Butterworth, Chebyshev, inverse Chebyshev, and Cauer parameter (elliptic) low-pass filters. using Darlington's results [11], [12] for avoiding the computation of elliptical (Jacobian) functions, easily manageable computation steps can be given which are simple enough for computations with certain pocket calculators. Design examples illustrate the efficiency of this design procedure. Finally, we will give a method which guarantees that these filters are scaled in the best possible way for sinusoidal excitation.

## II. Derivation of the Explicit Formulas

### 2.1. Basic Definitions

The basic principles of the lattice WDF's have been described in the literature [3]–[10], they will not be repeated here. Only the basic definitions will now be recalled.

The WDF's are derived from real lossless reference filters using the voltage wave quantities [1]. For a lattice WDF [3] the reference filter is a real symmetric two-port

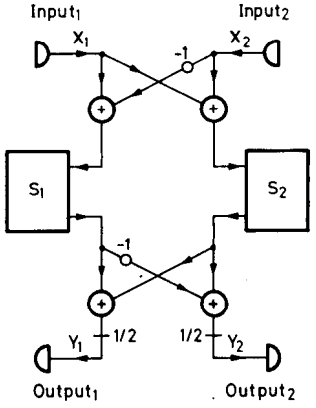


Fig. 1. Wave-flow diagram of a lattice WDF.

equally resistively terminated. The reference filter is designed in the $\psi$-domain, i.e., the complex frequency variable $\psi$ is used instead of the usual variable $p$. The relation between $\psi$ and $p$ is given by

$$\psi = \tanh pT/2 \tag{1a}$$

$$T = 1/F \tag{1b}$$

where $F$ is the sampling frequency.

In both lattice branches of the lattice WDF (see Fig. 1) $S_1(\psi)$ and $S_2(\psi)$ are reflectances of reactances, i.e., all-pass functions.

Consequently, they may be written (except for possible sign reverals) in the following form:

$$S_1 = \frac{g_1(-\psi)}{g_1(\psi)} \tag{2a}$$

and

$$S_2 = \frac{g_2(-\psi)}{g_2(\psi)} \tag{2b}$$

where $g_1(\psi)$ and $g_2(\psi)$ are Hurwitz polynomials [13] of degree $N_1$ and $N_2$, respectively.

Further, it is well known that the transfer functions which are realized by these WDF's are given by

$$S_{11} = S_{22} = \frac{S_1 + S_2}{2} = \frac{h(\psi)}{g(\psi)} \tag{3}$$

$$S_{21} = S_{12} = \frac{S_2 - S_1}{2} = \frac{f(\psi)}{g(\psi)} \tag{4}$$

where $h(\psi)$, $f(\psi)$, and $g(\psi)$ are the so-called canonic polynomials [13], [14].

We consider in the following the high-pass (or low-pass) case, and we will suppose that $N_1$ is odd and $N_2$ is even. The opposite choice would simply amount to changing the sign of (4) and this possibility can thus henceforth be ignored. Interchanging of $g_1(\psi)$ and $g_2(\psi)$ in (2) would simply lead to the dual realization, therefore, this possibility will also be ignored.

From (2), (3), or (4) we can see that

$$g(\psi) = g_1(\psi) \cdot g_2(\psi) \tag{5}$$

i.e., $g(\psi)$ is a Hurwitz polynomial of degree $N$ where

$N = N_1 + N_2$. Consequently, $N$ must be always an odd number for the high-pass (low-pass) filters. The degree of the lattice WDF [3] is the sum of the degrees of the two reflectances $S_1$ and $S_2$.

Further, from (2), (3), and (4) it is clear that

$$h(\psi) = \tfrac{1}{2}\{g_1(-\psi)g_2(\psi) + g_1(\psi)g_2(-\psi)\} \quad (6)$$

and

$$f(\psi) = \tfrac{1}{2}\{g_1(\psi)g_2(-\psi) - g_1(-\psi)g_2(\psi)\} \quad (7)$$

i.e., $h(\psi)$ and $f(\psi)$ are even and odd polynomials, respectively.

It is known, that the transfer functions are related at real frequencies $\psi = j\varphi$ by the Feldkeller equation [13]

$$|S_{11}(j\varphi)|^2 + |S_{21}(j\varphi)|^2 = 1. \quad (8)$$

The attenuation (or loss) is defined by

$$a(\varphi) = -20\log|S_{21}(j\varphi)|. \quad (9)$$

The so-called characteristic function is defined by

$$C(\psi) = \frac{S_{11}(\psi)}{S_{21}(\psi)} = \frac{h(\psi)}{f(\psi)}. \quad (10)$$

Further, it is clear that the zeros of the polynomial $g(\psi)g(-\psi)$ occur when

$$C^2(\psi) = 1. \quad (11)$$

From (6) and (7) we have

$$h(\psi) + f(\psi) = g_1(\psi)\cdot g_2(-\psi).$$

Accordingly, this equation implies that solving

$$C(\psi) = -1 \quad (12)$$

the polynomials $g_1(\psi)$ and $g_2(-\psi)$ can be constructed. Similarly, we can conclude that the solution of

$$C(\psi) = 1 \quad (13)$$

determines the polynomials $g_2(\psi)$ and $g_1(-\psi)$.

In the most common cases, i.e., in Butterworth, Chebyshev, inverse Chebyshev and Cauer parameter (elliptic) reference filters the equations (11)–(13) can be explicitly solved. Consequently, we can write the polynomials $g_1(\psi)$ and $g_2(\psi)$ in closed form.

Before attempting to determine the explicit formulas arising in the synthesis procedure we will discuss a certain property on the location of the zeros of polynomials $g_1(\psi)$ and $g_2(\psi)$ in the aforementioned cases.

### 2.2. *Alternating Distribution of Poles Among the Lattice Branches*

A simple proof for the fact that the poles of $S_{21}(\psi)$ are alternately distributed in a cyclic manner (see Fig. 2) among the lattice branches can be given comparing the solutions of (12), (13) to that of (11), which can be done explicitly for elliptic filters. In order to solve these equations we will adopt the approach used by Rhodes [15] for the high-pass elliptic prototype filter.

For these filters we have

$$C(\psi) = \frac{j}{\varepsilon \cdot F_N(-j\psi)} \quad (14)$$

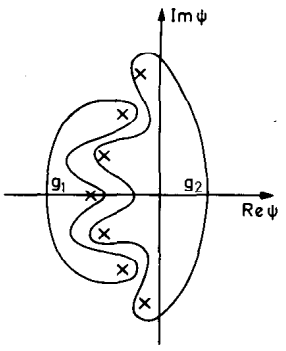


Fig. 2. Alternating distribution of the roots of the polinomials $g_1$ and $g_2$ (for $N = 7$).

where $F_N$ is a real rational function of degree $N$ and $\varepsilon$ is the ripple factor. The $F_N(\psi)$ may be expressed in the form

$$F_N(\psi) = cd_0\left\{\frac{N\cdot K(m_0)}{K(m)} cd^{-1}(-j\psi)\right\} \quad (15)$$

where the elliptic function $cd_0$ dependent upon the elliptic parameter $m_0$ has the quarter real period $K(m_0)$ and the inverse elliptic function $cd^{-1}$ dependent upon the elliptic parameter $m$ has the quarter real period $K(m)$.

Further, it is well known that the conditional requirement [15]

$$N\cdot\frac{K_0}{K} = \frac{K_0^x}{K^x}$$

has to be satisfied, where for the sake of simplicity we use the brief forms of $K_0 = K(m_0)$ and $K = K(m)$ with the complementary quarter periods $K_0^x$ and $K^x$, respectively.

From (14), (12) can be written as

$$F_N(\psi) = -\frac{j}{\varepsilon}. \quad (16)$$

Now, we define an auxiliary parameter $\eta$ as

$$j\eta = sn\left(\frac{K}{NK_0}\cdot sn_0^{-1}\frac{j}{\varepsilon}\right) \quad (17)$$

where the elliptic function $sn$ depends on the parameter $m$ and the inverse function $sn_0^{-1}$ depends on $m_0$.

Using (15) and (17), (16) may be written in the form

$$cd_0\left(\frac{NK_0}{K} cd^{-1} - j\psi\right) = -sn_0\left(\frac{NK_0}{K} sn^{-1} j\eta\right).$$

Solving this equation,

$$\frac{NK_0}{K} cd^{-1} - j\psi = \frac{NK_0}{K} sn^{-1} j\eta + (4r+1)K_0 + j2qK_0^x$$

where $r$ and $q$ are integers.

Accordingly, the zeros of $g_1(\psi)g_2(-\psi)$ occur at

$$\psi = -jcd\left(sn^{-1} j\eta + \frac{(4r+1)K}{N}\right),$$

$$\text{for } r = 0,1,\cdots,(N-1). \quad (18)$$

Repeating the procedure once again for (13) we can conclude that the zeros of $g_2(\psi)g_1(-\psi)$ occur at

$$\psi = -jcd\left(sn^{-1} j\eta + \frac{(4r-1)K}{N}\right), \quad \text{for } r = 1,2,\cdots,N. \quad (19)$$

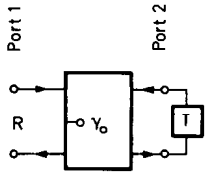


Fig. 3. Wave-flow diagram of an all-pass section of degree one.

Finally, solving (11) and selecting the roots of the left half-plane we have the zeros of $g_1(\psi)g_2(\psi)$ occur at [15]

$$\psi = -jcd\left(sn^{-1}j\eta + \frac{(2l-1)K}{N}\right), \qquad \text{for } l=1,2,\cdots,N. \tag{20}$$

Comparing (18) and (19) to (20) we can conclude that for $l$ odd and even, (20) gives the same values as (18) and (19), respectively, i.e., the zeros of $g_1(\psi)$ and $g_2(\psi)$ will lie in alternating order in the left half-plane of the complex frequency (see Fig. 2).

Since the inverse Chebyshev, the Chebyshev, and also the Butterworth case can be derived as limiting cases of elliptic function prototype filters [17], it is clear that this alternating property remains true also for these filter types.

### 2.3. Synthesis Using Cascaded All-Pass Functions

An all-pass function can be synthesized by several methods [3]–[6]. In this paper we will consider the realization as a cascade of elementary sections by means of three-port circulators [1].

The elementary sections are the first- and second-degree all-pass sections. A section of degree one has a reflectance of the following form:

$$S = \frac{-\psi + B_0}{\psi + B_0}$$

and a corresponding signal-flow diagram of a wave digital realization using the so-called two-port adaptor is given in Fig. 3 where the multiplier coefficient is given by [1], [6]

$$\gamma_0 = \frac{1-B_0}{1+B_0}. \tag{21}$$

A second-degree all-pass section has a reflectance of the form

$$S = \frac{\psi^2 - A_i\psi + B_i}{\psi^2 + A_i\psi + B_i}$$

and using the two-port adaptors the corresponding wave digital realization has equivalent wave-flow diagrams given by Fig. 4, where the coefficient values are given by [1], [6]

$$\gamma_{2i-1} = \frac{A_i - B_i - 1}{A_i + B_i + 1} \tag{22}$$

and

$$\gamma_{2i} = \frac{1-B_i}{1+B_i}. \tag{23}$$

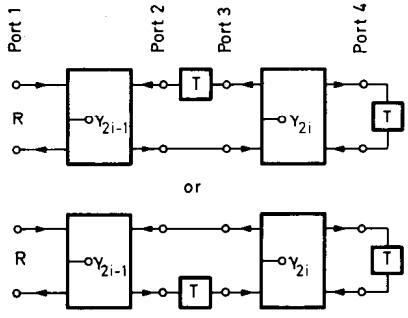


Fig. 4. Equivalent wave-flow diagrams of the $i$th second-degree all-pass section.

Now, let $g(\psi)$ be given in a product form

$$g(\psi) = (\psi + B_0)\prod_{i=1}^{(N-1)/2}\left(\psi^2 + \psi\cdot A_i + B_i\right). \tag{24}$$

When we utilize the alternating property relating to the distribution of the zeros of polynomials $g_1(\psi)$ and $g_2(\psi)$, all adaptor coefficients can be computed by (21), (22), and (23) from the parameters in (24). The corresponding block diagram for the filter is given in Fig. 5.

Since in the most common cases, i.e., in Butterworth, Chebyshev, inverse Chebyshev and Cauer parameter (elliptic) reference filters, (24) is given in closed form, the construction of explicit formulas is straightforward.

### 2.4. Derivation of Explicit Formulas

The derivation of the explicit formulas will be demonstrated by the most simple Butterworth (maximally flat) filter. It is well-known that in this case (24) has the following form [15]:

$$g(\psi) = (\psi + \varphi_0)\prod_{i=1}^{(N-1)/2}\left\{\psi^2 + 2\psi\varphi_0\cos(\pi i/N) + \varphi_0^2\right\}$$

where the passband edge (3.01 dB attenuation loss) frequency has the value

$$\varphi = \varphi_0.$$

Using (1) for $\psi = j\varphi$ and $p = j2\pi f$, we may write

$$\varphi_0 = \tan(\pi f_0/F).$$

Consequently, from (21), (22), and (23) we have for the coefficients

$$\gamma_0 = \frac{1-\tan(\pi f_0/F)}{1+\tan(\pi f_0/F)}$$

$$\gamma_{2i-1} = \frac{\sin(2\pi f_0/F)\cdot\cos(\pi i/N) - 1}{\sin(2\pi f_0/F)\cdot\cos(\pi i/N) + 1}, \qquad \text{for } i=1,2,\cdots,(N-1)/2$$

and

$$\gamma_2 = \gamma_4 = \cdots = \gamma_{N-1} = \cos(2\pi f_0/F). \tag{25}$$

The block diagram of the filter is shown in Fig. 5. To realize this filter we need $N$ delays, $(3N+1)$ adders (plus one adder if we use the complementary output for branching filters), $N$ multipliers and one (or two for branching filters) simple scalers with the factor 1/2.

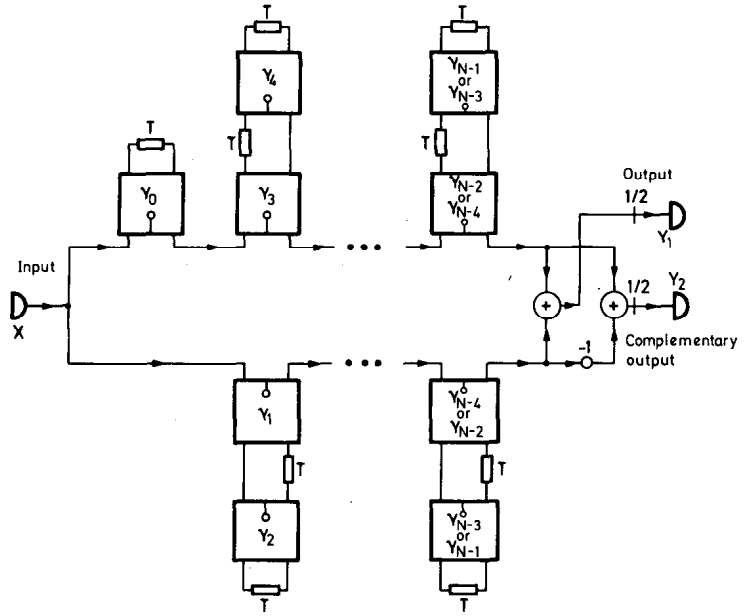


Fig. 5. Block diagram of the lattice WDF with cascaded all-pass sections for $N = 5,9,13,\cdots$, or $N = 7,11,15,\cdots$, respectively.

In the above explicit formulas the design parameters are the 3-dB frequency $f_0$ in the digital domain, the sampling frequency $F$, and the degree $N$ of the filter. However, the input parameters are usually given, as illustrated in Fig. 6, where $f_p$ and $f_s$ are the desired passband and stopband edges, $F$ is the sampling frequency, $a_p$ is the maximum passband loss, and $a_s$ is the minimum stopband loss (see (9)) for definition of loss). Of course, from these parameters the minimum value of the filter degree can easily be estimated (see Sections 3.1 and 3.2) and also a range for the allowable values of $f_0/F$ can be calculated. Furthermore, we can observe from (25) that in this case all even numbered coefficients have the same value, say $\gamma$, and this value can be arbitrarily chosen in a given range according to the allowable values of $f_0/F$. This fact suggests that $\gamma$ should be chosen as design parameter instead of $f_0$. Indeed, in Section 3.3 we will present the upper and lower bounds for $\gamma$ in terms of the input parameters, and we will give explicit formulas for the coefficient values in terms of $\gamma$ and $N$. Accordingly, we can usually choose $\gamma$ between its bounds in such a way that a simple value is obtained (the simplest being the choice $\gamma = 2^{-n}$, with $n$ integer; cf. the Appendix, Example 2). This method alleviates considerably the discrete optimization procedure since $(N-1)/2$ coefficients can be quantized by an appropriate choice during the design process.

For the other approximation types, (25) or a similar equation does not hold in general. Consequently, there is no reason for choosing any particular coefficient as design parameter. We will thus adopt the so-called ripple factor as well as $N$ as design parameters (see Sections 3.4 and 3.6). Starting from the parameters $B_0$, $A_i$, and $B_i$ occuring in (24), the construction of explicit formulas for Chebyshev and elliptic filters proceeds in the same way as for Butterworth filters. For determining $B_0$, $A_i$, and $B_i$, we use results given in [16], [18], [32]. In order to avoid the use of

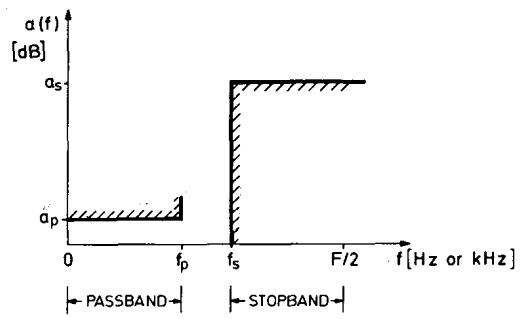


Fig. 6. Design specifications for low-pass filters.

the esoteric elliptic functions in the design of elliptic response filters we have adopted a method proposed by Darlington [11], [12]. This excellent method leads to an elegant and rapid way of designing elliptic filters (see the filter degree approximation in Section 3.2, the determination of the design margin and coefficient values in Section 3.6). As we will see in Section III, all design steps can be calculated by a pocket calculator without need for using filter catalogs [18]–[21] or writing intricate computer programs [22]–[24].

### 2.5. *Special Structure*

A very important subclass of lattice WDF's is formed by the filters with bireciprocal (also called, self-reciprocal [10]) characteristic function [7]. For these, the following property holds:

$$C(\psi) = \frac{1}{C(1/\psi)}. \tag{26}$$

An attenuation of 3.01 dB is then always obtained at one quarter of the sampling frequency. Furthermore, e.g., in the case of low-pass filters, only either the passband or the stopband attenuation can be freely prescribed since the attenuation in the range from 0 to $F/4$ is not independent

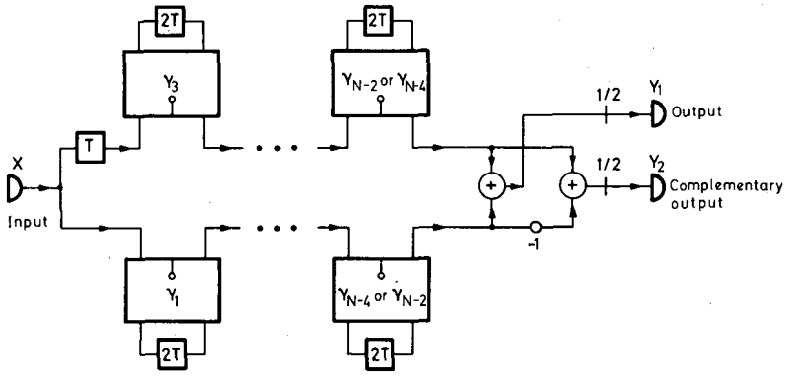


Fig. 7. Block diagram of the bireciprocal lattice WDF with cascaded all-pass sections for $N = 5,9,13,\cdots$, or $N = 7,11,15,\cdots$, respectively.

of that in the range from $F/4$ to $F/2$. It is known that these filters comprise only $(N-1)/2$ adaptors [7], i.e., less than half as many as usual lattice WDF's.

The block diagram of these filters is particularly simple (see Fig. 7). Furthermore, they have some important advantages: in the case of interpolation or decimation with a factor of two, the sampling rate alteration can be implemented very economically in a bireciprocal lattice WDF [8], [31]; they are optimally scaled for sinusoidal input signals (see Section 3.7, also [10]); simple two's complement value truncation is sufficient instead of magnitude truncation to guarantee freedom of zero input granular limit cycles (see also [10]); and these filters are well suited for realizing Nyquist pulse shapers [10].

For the explicit formulas, the condition (26) implies possibilities for simplifications; these will be mentioned at those places where they arise in describing the design of Butterworth and elliptic response filters (Chebyshev and inverse Chebyshev response shapes are not possible for this type of filter).

## III. Filter Design

We note that the following design procedure may be used directly even without fully understanding the methods used to obtain them.

### 3.1. Notation

The design specifications for a low-pass filter are frequently given as illustrated in Fig. 6, where,

- $a_s$ specified minimum attenuation in the stopband in decibels,
- $a_p$ maximum allowable attenuation spread in the passband in decibels,
- $f_s$ lower edge frequency of the stopband,
- $f_p$ upper edge frequency of the passband,
- $F$ sampling frequency.

Instead of the above parameters, the ripple factors $\varepsilon_s$, $\varepsilon_p$ and the transformed frequencies $\varphi_s$, $\varphi_p$ are more convenient to use in the explicit formulas. These are defined by

$$\varepsilon_s = \sqrt{10^{a_s/10} - 1} \tag{27a}$$

$$\varepsilon_p = \sqrt{10^{a_p/10} - 1} \tag{27b}$$

and

$$\varphi_s = \tan(\pi f_s/F) \tag{28a}$$

$$\varphi_p = \tan(\pi f_p/F). \tag{28b}$$

Accordingly, we have,

$$a_s = 10\log(1+\varepsilon_s^2) \tag{29a}$$

$$a_p = 10\log(1+\varepsilon_p^2) \tag{29b}$$

and

$$f_s = \frac{F}{\pi}\arctan\varphi_s \tag{30a}$$

$$f_p = \frac{F}{\pi}\arctan\varphi_p. \tag{30b}$$

### 3.2. Filter Degree

The first step in the design of a practical filter is the determination of the filter degree (order) $N$ required to meet the specifications.

A minimum value for the degree of the low-pass filter can be estimated by using the following approximations:

$$n_{\min} = \frac{c_1 \cdot \ln(c_2 \cdot \varepsilon_s/\varepsilon_p)}{\ln(c_3)} \tag{31}$$

where $c_1$, $c_2$, and $c_3$ are given in Table I with

$$k_0 = \sqrt{\varphi_s/\varphi_p} \tag{32a}$$

and

$$k_{i+1} = k_i^2 + \sqrt{k_i^4 - 1}, \qquad \text{for } i = 0,1,2,3. \tag{32b}$$

Note that in practice the values of $k_i$ for $i > 4$ are not needed [12]. The value of $n_{\min}$ is not necessarily an odd number. Taking the smallest odd $N$ satisfying

$$N \geq n_{\min} \tag{33}$$

a certain margin remains for the design parameters. This margin can be utilized in the procedure of quantizing the coefficients into fixed-point values (e.g., by simply rounding or by more involved discrete optimization algorithms [3], [5], [24]–[30]).

It is well known that in the passband, lattice WDF's have excellent sensitivity properties with respect to changes

TABLE I
PARAMETERS FOR APPROXIMATION OF THE DEGREE

| Filter type | $c_1$ | $c_2$ | $c_3$ |
|---|---|---|---|
| Butterworth (maximally flat) | 1 | 1 | $k_o^2$ |
| Chebyshev and inverse Chebyshev | 1 | 2 | $k_1$ |
| Cauer parameter (elliptic) | 8 | 4 | $2k_4$ |

in the multiplier coefficients, but that they have poor sensitivity properties in the stopband [3]–[6]. Therefore, the quantization procedure can be alleviated if the major part of the available design margin is allocated to the stopband.

### 3.3. Butterworth (Maximally Flat) Filters

*Determination of the Design Margin:*

Define the auxiliary parameters by

$$k_p = \frac{\sqrt[N]{\varepsilon_p^2 - \varphi_p^2}}{\sqrt[N]{\varepsilon_p^2 + \varphi_p^2}} \tag{34a}$$

and

$$k_s = \frac{\sqrt[N]{\varepsilon_s^2 - \varphi_s^2}}{\sqrt[N]{\varepsilon_s^2 + \varphi_s^2}}. \tag{34b}$$

Now, we can choose an arbitrary value for $\gamma$ which satisfies the inequalities

$$k_s \leqslant \gamma \leqslant k_p. \tag{35}$$

We note that the inequality $k_s \leqslant k_p$ follows in a simple manner from (31), (33), and (34). If we choose $\gamma = k_p$, the whole design margin will be allocated to the stopband, and in the case $\gamma = k_s$, to the passband.

If $k_s \leqslant 0$ and $0 \leqslant k_p$, we can choose $\gamma = 0$, which leads to the bireciprocal case.

*Determination of the Coefficient Values:*

Having chosen $\gamma$ in an appropriate way, the multiplier values are given by the expressions listed hereafter:

$$\gamma_0 = \frac{1+\gamma-\sqrt{1-\gamma^2}}{1+\gamma+\sqrt{1-\gamma^2}} \tag{36}$$

$$\gamma_{2i-1} = \frac{\sqrt{1-\gamma^2}\cdot\cos(\pi i/N)-1}{\sqrt{1-\gamma^2}\cdot\cos(\pi i/N)+1} \tag{37a}$$

$$\gamma_{2i} = \gamma \tag{37b}$$

thus in the bireciprocal case,

$$\gamma_0 = 0, \quad \gamma_{2i-1} = -\tan^2(\pi i/2N), \quad \gamma_{2i} = 0 \tag{38}$$

respectively, with $i = 1,2,\cdots,(N-1)/2$. The block diagram of the filter is shown in Fig. 5, and for the bireciprocal case in Fig. 7.

### 3.4. Chebyshev Filters

*Determination of the Design Margin:*

We can compute the smallest possible value of the passband ripple factor by

$$\varepsilon_{p\min} = \frac{2\varepsilon_s}{k_1^N} \tag{39}$$

where $k_1$ is given by (32).

Accordingly, we can choose an actual passband ripple factor $\varepsilon_p^*$ in such a way that its value satisfies the inequalities

$$\varepsilon_{p\min} \leqslant \varepsilon_p^* \leqslant \varepsilon_p. \tag{40}$$

We note that the inequality $\varepsilon_{p\min} \leqslant \varepsilon_p$ follows from (31), (33), and (39). If we choose $\varepsilon_p^* = \varepsilon_p$, the whole design margin will be allocated to the stopband, and in the case $\varepsilon_p^* = \varepsilon_{p\min}$, to the passband.

*Determination of the Coefficient Values:*

In terms of $\varepsilon_p^*$ we define further auxiliary parameters as follows:

$$w = \sqrt[N]{\frac{1}{\varepsilon_p^*} + \sqrt{\frac{1}{\varepsilon_p^{*2}} + 1}} \tag{41}$$

and

$$r = \left(w - \frac{1}{w}\right)\cdot\varphi_p. \tag{42}$$

Then, the multiplier values are given by

$$\gamma_0 = \frac{2-r}{2+r} \tag{43}$$

$$\gamma_{2i-1} = \frac{A_i - B_i - 1}{A_i + B_i + 1} \tag{44}$$

$$\gamma_{2i} = \frac{1-B_i}{1+B_i} \tag{45}$$

where

$$A_i = r\cdot\cos(\pi i/N) \tag{46}$$

$$B_i = \left\{w^2 + \frac{1}{w^2} - 2\cos(2\pi i/N)\right\}\varphi_p^2/4 \tag{47}$$

with $i = 1,2,\cdots,(N-1)/2$.

The block diagram of the filter is shown in Fig. 5.

### 3.5. Inverse Chebyshev Filters

We can observe from (8) that the function $|S_{11}(j\varphi)|$ has an inverse Chebyshev high-pass filter response, if the transfer function $|S_{21}(j\varphi)|$ has Chebyshev low-pass response. Accordingly, using appropriate frequency transformations an inverse Chebyshev low-pass filter can be very easily derived from a suitable Chebyshev low-pass filter.

### 3.6. Cauer Parameter (Elliptic) Filters

*Determination of the Design Margin:*

In this case we will split the design margin among three intervals: the passband, the stopband, and the transition band.

Now, we will choose the actual value of the lower stopband edge frequency $f_s^*$ and the actual value of the passband ripple factor $\varepsilon_p^*$, while the actual value of the stopband ripple factor $\varepsilon_s^*$ will be obtained during the calculation process.

We define the auxiliary parameters by means of

$$r_0 = \sqrt{\varepsilon_s/\varepsilon_p} \tag{48a}$$

thus in the bireciprocal case

$$r_0 = \varepsilon_s \tag{48b}$$

and furthermore,

$$r_{i+1} = r_i^2 + \sqrt{r_i^4 - 1}, \qquad \text{for } i = 0,1 \tag{49}$$

$$x_4 = \frac{1}{2}\left(\sqrt[N]{2r_2}\right)^4 \tag{50}$$

$$x_{i-1} = \sqrt{\frac{1}{2}\left(x_i + \frac{1}{x_i}\right)}, \qquad \text{for } i = 4,3,2,1. \tag{51}$$

Then the minimum value of the lower stopband edge frequency can be computed by

$$f_{s\min} = \frac{F}{\pi}\arctan \varphi_p x_0^2 \tag{52a}$$

thus in the bireciprocal case,

$$f_{s\min} = \frac{F}{\pi}\arctan x_0. \tag{52b}$$

Accordingly, we can choose the actual value for $f_s^*$ which satisfies the inequalities

$$f_{s\min} \leqslant f_s^* \leqslant f_s. \tag{53}$$

We note that the choice $f_s^* = f_{s\min}$ would allocate the entire design margin to the transition band, and $f_s^* = f_s$, to the passband and stopband.

Assuming $f_s^*$ to be chosen in an appropriate way, we will discuss how to split the remaining design margin among the passband and stopband.

We compute using (28a)

$$\varphi_s^* = \tan\left(\pi f_s^*/F\right) \tag{54}$$

then we have

$$q_0 = \sqrt{\varphi_s^*/\varphi_p}. \tag{55a}$$

thus in bireciprocal case,

$$q_0 = \varphi_s^* \tag{55b}$$

and furthermore,

$$q_{i+1} = q_i^2 + \sqrt{q_i^4 - 1}, \qquad \text{for } i = 0,1,2,3, \tag{56}$$

$$m_3 = \frac{1}{2}\left(\sqrt{2q_4}\right)^N \tag{57}$$

$$m_{i-1} = \sqrt{\frac{1}{2}\left(m_i + \frac{1}{m_i}\right)}, \qquad \text{for } i = 3,2,1. \tag{58}$$

Then, we can compute the smallest possible value of the passband ripple factor by

$$\varepsilon_{p\min} = \frac{\varepsilon_s}{m_0^2} \tag{59a}$$

thus in the bireciprocal case,

$$\varepsilon_{p\min} = \frac{1}{m_0}. \tag{59b}$$

Accordingly, we can choose the actual value $\varepsilon_p^*$ which satisfies the inequalities

$$\varepsilon_{p\min} \leqslant \varepsilon_p^* \leqslant \varepsilon_p. \tag{60}$$

We note that the choice $\varepsilon_p^* = \varepsilon_{p\min}$ would allocate the entire design margin to the passband, and $\varepsilon_p^* = \varepsilon_p$, to the stopband. Assuming $\varepsilon_p^*$ to be chosen in an appropriate way the actual value of the stopband ripple factor $\varepsilon_s^*$ can be calculated by

$$\varepsilon_s^* = \varepsilon_p^* \cdot m_0^2 \tag{61a}$$

thus in the bireciprocal case,

$$\varepsilon_s^* = m_0. \tag{61b}$$

We note that the inequalities $\varepsilon_s \leqslant \varepsilon_s^*$, $f_{s\min} \leqslant f_s$, and $\varepsilon_{p\min} \leqslant \varepsilon_p$ can be easily proven.

*Determination of the Coefficient Values:*

We define auxiliary parameters by means of

$$g_1 = \frac{1}{\varepsilon_p^*} + \sqrt{\frac{1}{\varepsilon_p^{*2}} + 1} \tag{62}$$

$$g_{i+1} = m_i g_i + \sqrt{(m_i g_i)^2 + 1}, \qquad \text{for } i = 1,2 \tag{63}$$

$$w_5 = \sqrt[N]{\frac{m_3}{g_3} + \sqrt{\left(\frac{m_3}{g_3}\right)^2 + 1}} \tag{64}$$

$$w_{i-1} = \frac{1}{2q_{i-1}}\left(w_i - \frac{1}{w_i}\right), \qquad \text{for } i = 5,4,3,2,1. \tag{65a}$$

In the bireciprocal case we have

$$w_0 = -1. \tag{65b}$$

Then, the value of the multiplier $\gamma_0$ is given by

$$\gamma_0 = \frac{1 + w_0 q_0 \varphi_p}{1 - w_0 q_0 \varphi_p} \tag{66a}$$

thus in the bireciprocal case,

$$\gamma_0 = 0. \tag{66b}$$

In order to calculate the other multiplier values we define auxiliary parameters for $i = 1,2,\cdots,(N-1)/2$

$$c_{4,i} = \frac{q_4}{\sin\dfrac{i\pi}{N}} \tag{67}$$

$$c_{j-1,i} = \frac{1}{2q_{j-1}}\left(c_{j,i} + \frac{1}{c_{j,i}}\right), \qquad \text{for } j = 4,3,2,1 \tag{68}$$

$$y_i = \frac{1}{c_{0,i}} \tag{69}$$

$$B_i = \frac{w_0^2 + y_i^2}{1 + (w_0 y_i)^2} \cdot (q_0 \varphi_p)^2 \tag{70a}$$

$$A_i = \frac{-2w_0 q_0 \varphi_p}{1 + (w_0 y_i)^2} \cdot \sqrt{1 - \left(q_0^2 + \frac{1}{q_0^2} - y_i^2\right) y_i^2} \tag{71a}$$

thus in the bireciprocal case

$$B_i = 1 \tag{70b}$$

$$A_i = \frac{2}{1+y_i^2}\sqrt{1-\left(q_0^2+\frac{1}{q_0^2}-y_i^2\right)y_i^2}\,. \tag{71b}$$

Then, the other multiplier values are for $i=1,2,\cdots,(N-1)/2$

$$\gamma_{2i-1} = \frac{A_i - B_i - 1}{A_i + B_i + 1} \tag{72a}$$

$$\gamma_{2i} = \frac{1-B_i}{1+B_i} \tag{73a}$$

thus in the bireciprocal case,

$$\gamma_{2i-1} = \frac{A_i - 2}{A_i + 2} \tag{72b}$$

$$\gamma_{2i} = 0. \tag{73b}$$

The block diagram of the filter is shown in Fig. 5 and for the bireciprocal case in Fig. 7.

*Critical Frequencies:*

We can easily calculate the critical frequencies in the stopband and the passband using the above results. The transmission zeros (see Fig. 8) are given by

$$f_{\infty,i} = \frac{F}{\pi}\arctan\left(q_0\varphi_p/y_i\right), \qquad \text{for } i=1,2,\cdots,(N-1)/2. \tag{74}$$

Similarly, the frequencies of zero passband loss (see also Fig. 8) are given by

$$f_{0,i} = \frac{F}{\pi}\arctan\left(q_0\varphi_p y_i\right), \qquad \text{for } i=1,2,\cdots,(N-1)/2. \tag{75}$$

*Accuracy:*

Darlington himself has already demonstrated that the method proposed by him [11], [12] has excellent accuracy properties if $q_4 > 100$. The author of the present paper can support this fact since a comparison of a large number of examples computed on the one hand by the formulae given above and on the other, for controlling purposes, by using the values given in the new design catalogue from Saal [21] leads to the following observation. Using a TI-59 pocket calculator, all results were in agreement even in the most critical cases ($N=15$) at least up to eight decimal digits. In general, this precision is more than needed in practice.

### 3.7. Dynamic Range

It is well-known that WDF's have inherently good dynamic range [2]. In this section we will see that lattice WDF's with lattice branches realized by cascaded first and second degree all-pass sections are scaled in the best possible way for a sinusoidal excitation. It can be shown [33] that using certain adaptor equivalences [34] the amplitudes of the internal signals at all ports (see Figs. 3 and 4) do not exceed the input level at steady-state conditions for any frequency. There exists, however, always a frequency, say

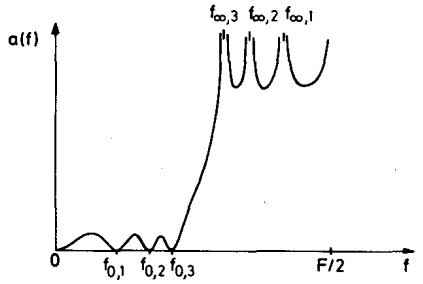


Fig. 8. The critical frequencies of a Cauer parameter (elliptic) filter (for $N=7$).

$f_m$, where the maximum just reaches the input level. This frequency is $f_m = 0$ or $F/2$ for a first degree section. For a second degree section we can prove that

$$f_m = \begin{cases} 0 \text{ or } F/2, & \text{if } \gamma_{2i-1} > 0 \\ \dfrac{F}{2\pi}\arccos\gamma_{2i}, & \text{if } \gamma_{2i-1} < 0 \end{cases}$$

is the frequency at which the signal levels at ports 2 and 3 (see Fig. 4) just reach the input level. The maximal signal level at port 4 (see Fig. 4) for unity input level is equal to

$$\begin{cases} 1, & \text{if } \gamma_{2i-1} > 0 \\ \sqrt{\dfrac{1-\gamma_{2i}}{1+\gamma_{2i}}}, & \text{if } \gamma_{2i-1} < 0 \text{ and } \gamma_{2i} > 0 \end{cases}$$

and

$$\sqrt{\frac{1+\gamma_{2i}}{1-\gamma_{2i}}}, \qquad \text{if } \gamma_{2i-1} < 0 \text{ and } \gamma_{2i} < 0.$$

Accordingly, bireciprocal filters are always scaled in the best possible way, and in the other cases (except for the very narrow band cases) nearly as well. In Fig. 9 are shown the signal-flow diagrams of the two-port adaptors which lead to this scaling. We can observe that a different structure has to be chosen depending on the multiplier value $\gamma$. Furthermore, we can see that the multiplier coefficient $\alpha$ which has to be implemented is always positive and not larger than one-half. Since we do not need additional scalers to achieve $L_\infty$ scaling [35] the designation "inherently scaled in the best possible way" seems to be appropriate for this type of filter.

### 3.8. Remarks

It should be stressed that WDF's represent a large family of digital filters since one can choose from a large number of reference filters each leading to a different structure [2]. From this family, we have discussed in this paper only one member, which represents an interesting and important structure; of course, this choice does not have to be optimal in all cases (e.g., for the narrow band case, there are more suitable WDF structures).

Even in the absence of any protective measures (except for the need of one or two guard bits inside of the adaptors for managing overflow [36], [37], WDF's tend to be almost free of limit cycle (parasitic) oscillations of either type, i.e., of overflow as well as granularity oscillations. Further-

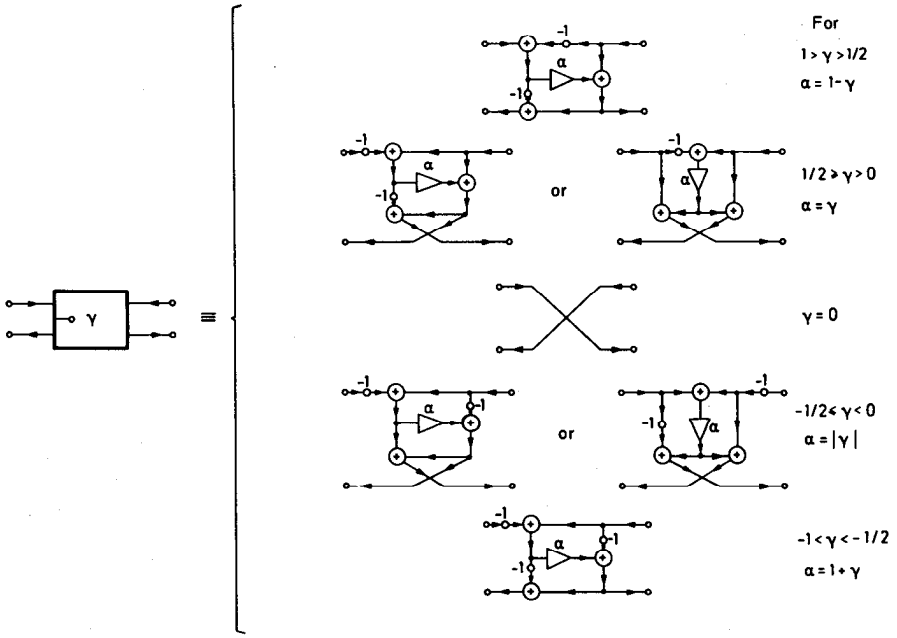


Fig. 9. Signal-flow diagrams of the two-port adaptor yielding optimal scaling for sinusoidal excitation. (Note that in the first diagram of the second last row, $\alpha$ should be replaced by $-\alpha$.)

more, it is well-known [38], [39] that saturation characteristics at the adaptor outputs guarantee forced response stability [40], that looped stability can be ensured [41], etc. For freedom from zero-input granularity limit cycles magnitude truncation of the state variables is usually sufficient [36]. In the bireciprocal case, however, it is easily shown (see also [10]) that simple two's complement value truncation is sufficient for zero input stability.

Furthermore, although we have restricted ourselves in this paper to designing low-pass filters, the design of a bandpass filter can be carried out in a straightforward manner using the usual network transformations [16], [18]–[21]. We note that a WDF is inherently a branching (bidirectional) filter, because not only the transmittances (4), but also the reflectances (3) are available as transfer functions, and these functions are complementary (see, e.g., (8)). This fact can be utilized to design high-pass and bandstop filters simply from proper low-pass and bandpass filters, respectively, using the complementary outputs in Figs. 5 or 7.

The design procedures described above will be illustrated hereafter in some detail by a number of examples. Although the design process has been simplified to the extent that a pocket calculator is sufficient for carrying out the necessary calculations, it is recommended to write a computer program for one's own use. In order to alleviate the debugging procedure the examples presented have been selected in such a way that most of the formulas presented above can be checked numerically at least once (see Appendix).

Finally, we have to stress that care must be taken not to confuse the lattice wave digital filters with the lattice digital filters as proposed by Gray and Markel [43]–[45]. Indeed, in the case of WDF's the term lattice refers to the structure of the reference filters, while in the Gray and Markel terminology it refers to the structure of the signal-flow diagram of the actual digital filter.

## IV. Conclusion

Digital filters are of great importance in digital signal processing systems. This paper was intended to aid the design engineer in solving most of his filter design problems without the need for the highly complex computations involved in network synthesis methods. We have seen that all design steps (starting from the design specifications, determination of the degree of the filter, manageing of the design margin, determination of the coefficient values, choosing signal-flow diagrams scaled in the best possible way) can be done in a simple top down way for lattice wave digital filters when both lattice branches were realized by cascaded first and second degree all-pass sections.

Accordingly, these filters with the proposed design method are very appropriate for using as input parts (specs to signal-flow diagram) in silicon compilers for digital filters [46]–[48] or in high level language programs for digital signal processors [49], [50].

## Appendix
## Numerical Examples

*Example 1*

Butterworth (maximally flat) low-pass filter:

*a) Requirements:*

| | | | |
|---|---|---|---|
| Passband: | $f_p = 3.4$ kHz | $a_p =$ | 0.5 dB |
| Stopband: | $f_s = 6$ kHz | $a_s =$ | 65 dB |
| Sampling frequency: | | $F =$ | 16 kHz. |

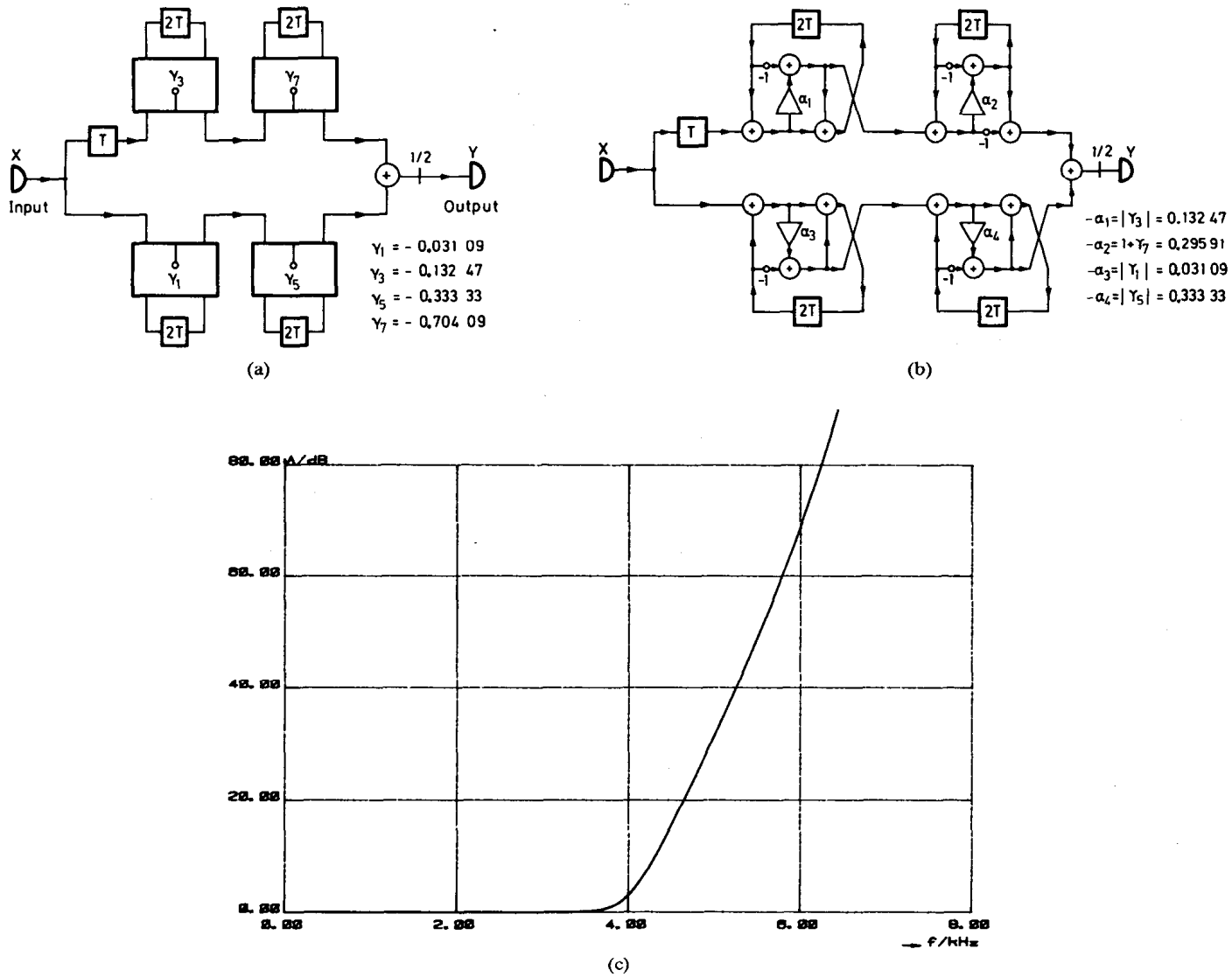


Fig. 10. Ninth degree bireciprocal WDF with Butterworth response. (a) Block diagram. (b) Signal-flow diagram. (c) Attenuation characteristic.

*b) Design procedure:*

Using (27), (28) the design parameters are given by

$$\varepsilon_s = \sqrt{10^{65/10} - 1} = 1778$$

$$\varepsilon_p = \sqrt{10^{0.5/10} - 1} = 0.3493$$

$$\varphi_s = \tan(\pi 6/16) = 2.414$$

$$\varphi_p = \tan(\pi 3.4/16) = 0.7883.$$

A *minimum degree* can be estimated by (31), and (32a)

$$n_{\min} = \frac{\ln(1778/0.3493)}{\ln(2.414/0.7883)} = 7.63.$$

This means we must choose minimum $N = 9$. Now, we compute the *auxiliary parameters* given by (34)

$$k_p = \frac{\sqrt[9]{0.3493^2 - 0.7883^2}}{\sqrt[9]{0.3493^2 + 0.7883^2}} = 0.1204$$

$$k_s = \frac{\sqrt[9]{1778^2 - 2.414^2}}{\sqrt[9]{1778^2 + 2.414^2}} = -0.0498.$$

Since $k_s < 0$ and $k_p > 0$ we can choose the bireciprocal case. The nonzero *coefficient values* from (38) are

$$\gamma_1 = -\tan^2(\pi/18) = -0.03109$$

$$\gamma_3 = -\tan^2(2\pi/18) = -0.13247$$

$$\gamma_5 = -\tan^2(3\pi/18) = -0.33333$$

$$\gamma_7 = -\tan^2(4\pi/18) = -0.70409.$$

In Fig. 10(a)–(c) we can see the block diagram, the signal-flow diagram with optimally scaled structure, and the computed attenuation characteristic of this filter, respectively.

*Example 2*

Butterworth (maximally flat) low-pass filter:

*a) Requirements:*

All requirements are the same as in Example 1 with the only exception: $a_s = 55$ dB.

*b) Design procedure:*

In this case from (27a) we have

$$\varepsilon_s = 562.3.$$

The other values of design parameters are the same as in Example 1.

The estimation of the *minimum degree* gives in this case

$$n_{\min} = 6.60$$

which means that $N = 7$ would be sufficient. Now, we compute the *auxiliary parameters*, we have

$$k_p = 0.087$$

and

$$k_s = 0.023.$$

We can conclude that now for $\gamma$ we can not choose the value zero (i.e., in this case we have not bireciprocal filter). However, we can observe that the choice

$$\gamma = \frac{1}{16} = 0.0625$$

satisfies (35) and gives simultaneously the larger part of the design margin to the stopband as was recommended. Further, this value leads to a very simple realization of the required multiplication.

Using this value for $\gamma$, the multiplier *coefficient values* are given by (36) and (37)

$$\gamma_0 = \frac{1+\frac{1}{16}-\sqrt{1-\left(\frac{1}{16}\right)^2}}{1+\frac{1}{16}+\sqrt{1-\left(\frac{1}{16}\right)^2}} = 0.03128$$

$$\gamma_1 = \frac{\sqrt{1-\frac{1}{16^2}}\cdot\cos(\pi/7)-1}{\sqrt{1-\frac{1}{16^2}}\cdot\cos(\pi/7)+1} = -0.05307$$

$$\gamma_3 = \frac{\sqrt{1-\frac{1}{16^2}}\cdot\cos(\pi 2/7)-1}{\sqrt{1-\frac{1}{16^2}}\cdot\cos(\pi 2/7)+1} = -0.23284$$

$$\gamma_5 = \frac{\sqrt{1-\frac{1}{16^2}}\cdot\cos(\pi 3/7)-1}{\sqrt{1-\frac{1}{16^2}}\cdot\cos(\pi 3/7)+1} = -0.63655$$

and

$$\gamma_2 = \gamma_4 = \gamma_6 = \frac{1}{16}.$$

In Fig. 11(a)–(c) we can see the block diagram, the signal-flow diagram with optimally scaled structure and the computed attenuation characteristic of this filter, respectively. We mention that in certain cases a realization with alternatively positioned delay elements (see Fig. 4) could be appropriate [42].

Comparing Fig. 10 to Fig. 11 we can observe that the structure in Fig. 10 is simpler than that in Fig. 11 in spite of the larger degree of the filter in Example 1. The simplicity of the structure in Example 1 follows from the fact that this filter has bireciprocal characteristic function.

*Example 3*

Chebyshev low-pass filter:

*a) Requirements:*

Passband: $f_p = 3$ kHz $a_p = 1$ dB

Stopband: $f_s = 5$ kHz $a_s = 40$ dB

Sampling frequency: $F = 16$ kHz.

*b) Design procedure:*

Using (27), (28) the design parameters are given by

$$\varepsilon_s = 99.995$$

$$\varepsilon_p = 0.5088$$

$$\varphi_s = 1.4966$$

$$\varphi_p = 0.668\,179.$$

A *minimum degree* can be estimated by (31) and (32)

$$k_1 = \frac{1.4966}{.66818} + \sqrt{\left(\frac{1.4966}{.66818}\right)^2 - 1} = 4.244$$

$$n_{\min} = \frac{\ln(2\cdot 99.995/0.5088)}{\ln 4.244} = 4.13.$$

This means we must choose minimum $N = 5$. Now, we compute the *design margin*. From (39) we have

$$\varepsilon_{p\,\min} = \frac{2\cdot 99.995}{(4.244)^5} = 0.145.$$

Let $\varepsilon_p^* = 0.4$ which corresponds from (29b) to

$$a_p^* = 10\log(1+0.4^2) = 0.645 \text{ dB}$$

and this choice satisfies (40) and splits the design margin according to the recommendation.

Then, the *auxiliary parameters* are given by (41), (42)

$$w = \sqrt[5]{\frac{1}{0.4}+\sqrt{\frac{1}{0.4^2}+1}} = 1.390198$$

$$r = \left(1.390198 - \frac{1}{1.390198}\right)\cdot 0.668179$$

$$= 0.448\,265.$$

Then the *coefficient value* $\gamma_0$ from (43) is given by

$$\gamma_0 = \frac{2-0.44827}{2+0.44827} = 0.6338.$$

For the other coefficient values we compute first

$$w^2 + \frac{1}{w^2} = 2.450075$$

$$\frac{1}{4}\varphi_p^2 = 0.111616$$

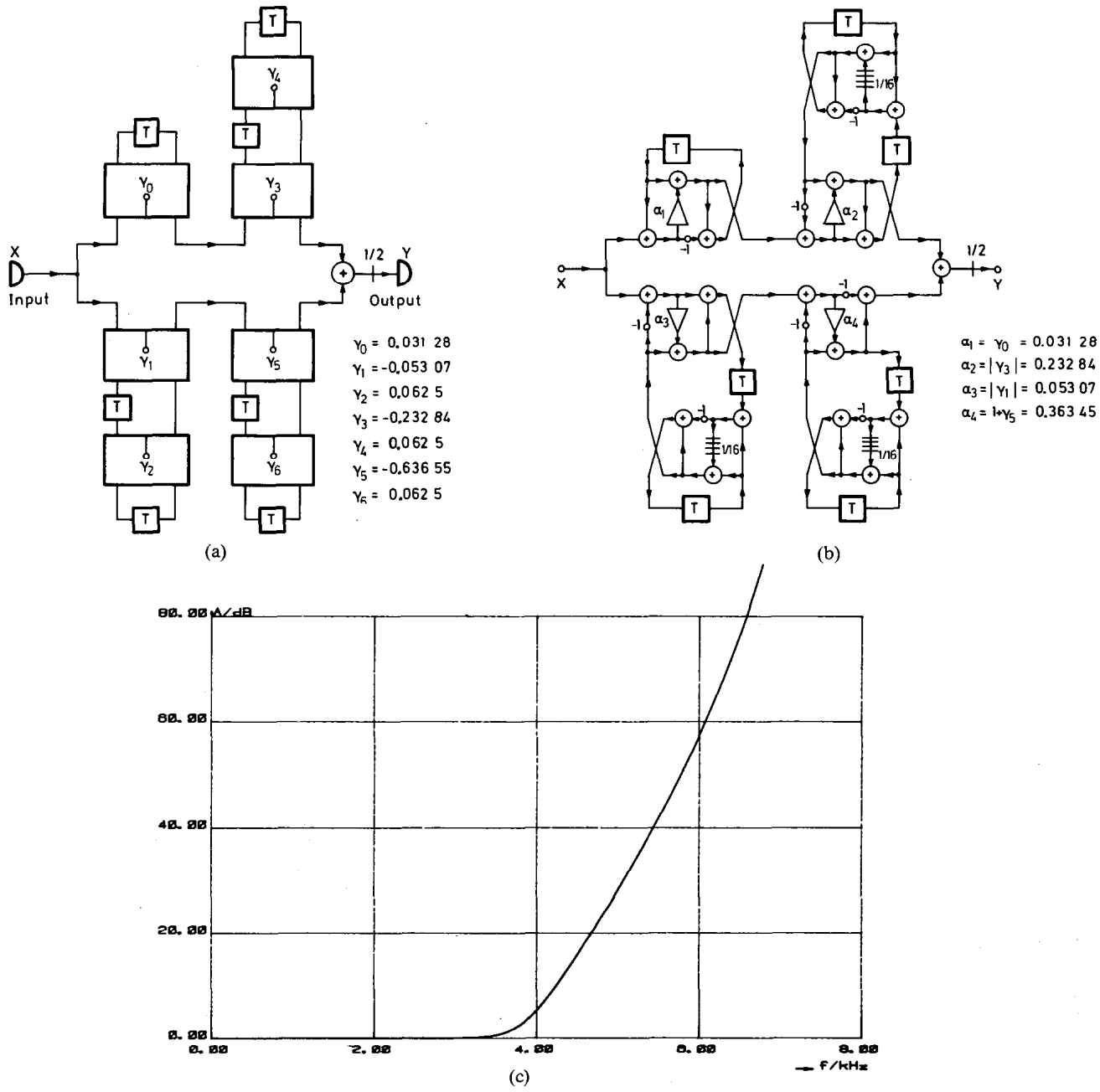


Fig. 11. Seventh degree WDF with Butterworth response. (a) Block diagram. (b) Signal-flow diagram. (c) Attenuation characteristic.

then, from (44), (45), (46) and (47) we have for $i=1$

$$A_1 = 0.448265 \cdot \cos(\pi/5) = 0.362654$$

$$B_1 = \{2.450075 - 2\cos(2\pi/5)\} \cdot 0.111616 = 0.204485$$

$$\gamma_1 = \frac{0.362654 - 0.204485 - 1}{0.362654 + 0.204485 + 1} = -0.5372$$

$$\gamma_2 = \frac{1 - 0.204485}{1 + 0.204485} = 0.6605$$

and for $i=2$

$$A_2 = 0.448265 \cdot \cos(2\pi/5) = 0.138522$$

$$B_2 = \{2.450075 - 2\cos(4\pi/5)\} \cdot 0.111616 = 0.454\,066$$

$$\gamma_3 = \frac{0.138522 - 0.454066 - 1}{0.138522 + 0.454066 + 1} = -0.8260$$

$$\gamma_4 = \frac{1 - 0.454066}{1 + 0.454066} = 0.3755.$$

In Fig. 12(a)–(d) we can see the block diagram, the signal-flow diagram with optimally scaled structure, the computed attenuation characteristic of this filter and the passband attenuation behavior, respectively.

*Example 4*

Cauer parameter (elliptic) low-pass filter:

*a) Requirements:*

| | | |
|---|---|---|
| Passband: | $f_p = 3.4$ kHz | $a_p = 0.2$ dB |
| Stopband: | $f_s = 4.6$ kHz | $a_s = 65$ dB |
| Sampling frequency: | | $F = 16$ kHz. |

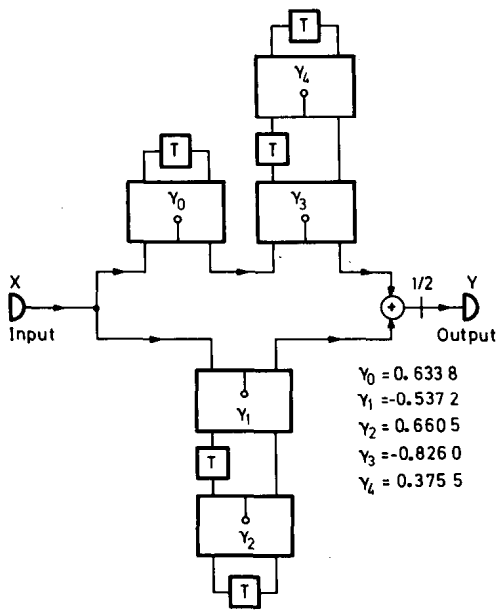


(a)

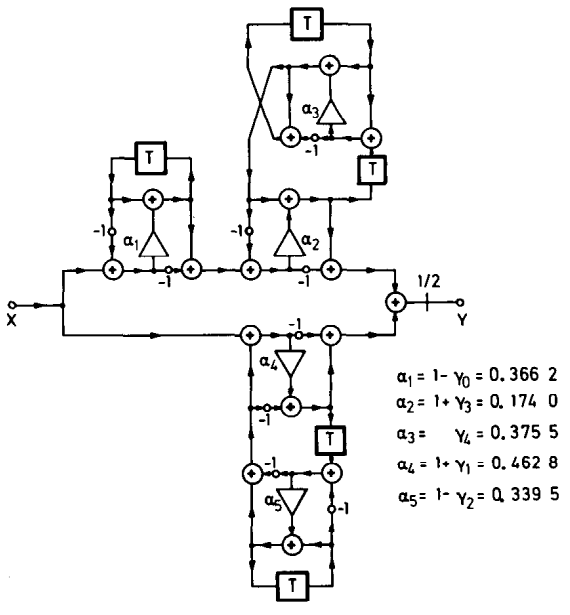


(b)

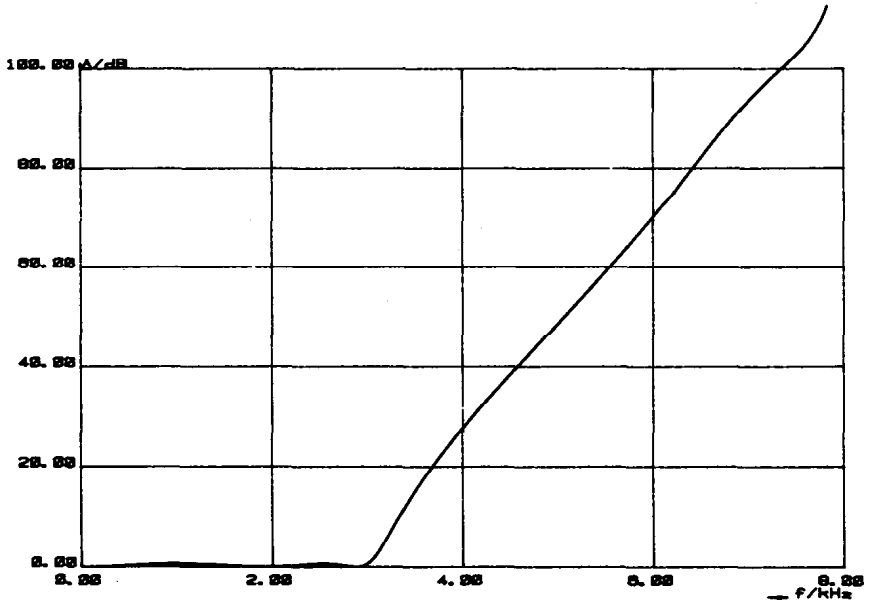


(c)

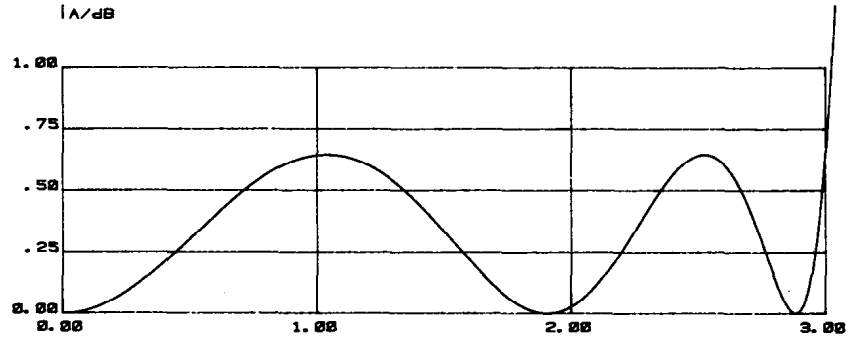


(d)

Fig. 12. Fifth degree WDF with Chebyshev response. (a) Block diagram. (b) Signal-flow diagram. (c) Attenuation characteristic. (d) Passband behavior.

*b) Design procedure:*
Using (27), (28) the design parameters are given by

$$\varepsilon_s = 1778.279\,129$$
$$\varepsilon_p = 0.217\,091\,1054$$
$$\varphi_s = 1.268\,493\,953$$
$$\varphi_p = 0.788\,336\,4346.$$

A *minimum degree* can be estimated by (31) and (32)

$$k_0 = \sqrt{\frac{1.268494}{0.788336}} = 1.268\,493\,95$$
$$k_1 = 1.26849395^2 + \sqrt{1.268494^4 - 1} = 2.869\,683$$
$$k_2 = 2.869683^2 + \sqrt{2.869683^4 - 1} = 16.409\,22$$
$$k_3 = 16.40922^2 + \sqrt{16.40922^4 - 1} = 538.523$$
$$k_4 = 538.523^2 + \sqrt{538.523^4 - 1} = 580014$$
$$n_{\min} = \frac{8 \cdot \ln(4 \cdot 1778/0.2171)}{\ln(2 \cdot 580014)} = 5.96.$$

This means we must choose minimum $N = 7$.
*Determination of the Design Margin:*
We compute the parameters from (48a), (49)–(51)

$$r_0 = \sqrt{\frac{1778.279129}{0.2170911054}} = 90.506\,329\,14$$
$$r_1 = r_0^2 + \sqrt{r_0^4 - 1} = 1.638\,279\,117 \times 10^4$$
$$r_2 = r_1^2 + \sqrt{r_1^4 - 1} = 5.367\,916\,929 \times 10^8$$
$$x_4 = \frac{1}{2}\left(\sqrt[7]{2r_2}\right)^4 = 7.235\,150\,91 \times 10^4$$
$$x_3 = \sqrt{\frac{1}{2}\left(x_4 + \frac{1}{x_4}\right)} = 190.199\,249\,6$$
$$x_2 = \sqrt{\frac{1}{2}\left(x_3 + \frac{1}{x_3}\right)} = 9.752\,038\,435$$
$$x_1 = \sqrt{\frac{1}{2}\left(x_2 + \frac{1}{x_2}\right)} = 2.219\,750\,11$$
$$x_0 = \sqrt{\frac{1}{2}\left(x_1 + \frac{1}{x_1}\right)} = 1.155\,476\,367.$$

Then the minimum value of stopband edge frequency from (52a)

$$f_{s\,\min} = \frac{16}{\pi} \arctan(0.788336 \cdot 1.155476^2) = 4.13 \text{ kHz},$$

i.e., we can choose an actual value for $f_s^*$ which satisfies

$$4.13 \leqslant f_s^* \leqslant 4.6.$$

Now, let $f_s^* = 4.5$ kHz. Then, we compute and store for later application the auxiliary parameters from (54), (55a), (56)–(58)

$$\varphi_s^* = \tan(\pi \cdot 4.5/16) = 1.218\,503\,526$$
$$q_0 = \sqrt{\frac{\varphi_s^*}{\varphi_p}} = 1.243\,247\,503$$
$$q_1 = q_0^2 + \sqrt{q_0^4 - 1} = 2.724\,256\,011$$
$$q_2 = q_1^2 + \sqrt{q_1^4 - 1} = 14.775\,461\,84$$
$$q_3 = q_2^2 + \sqrt{q_2^4 - 1} = 4.366\,262\,551 \times 10^2$$
$$q_4 = q_3^2 + \sqrt{q_3^4 - 1} = 3.812\,849\,732 \times 10^5$$
$$m_3 = \frac{1}{2}\left(\sqrt{2q_4}\right)^7 = 1.936\,194\,1 \times 10^{20}$$
$$m_2 = \sqrt{\frac{1}{2}\left(m_3 + \frac{1}{m_3}\right)} = 9.839\,192\,415 \times 10^9$$
$$m_1 = \sqrt{\frac{1}{2}\left(m_2 + \frac{1}{m_2}\right)} = 7.013\,983\,324 \times 10^4$$
$$m_0 = \sqrt{\frac{1}{2}\left(m_1 + \frac{1}{m_1}\right)} = 187.269\,636\,2.$$

The available minimum value of the passband ripple factor from (59a)

$$\varepsilon_{p\,\min} = \frac{1778.279}{187.2696^2} = 0.0507$$

i.e., we can choose an actual $\varepsilon_p^*$ satisfying (60):

$$0.0507 \leqslant \varepsilon_p^* \leqslant 0.2.$$

Now, we choose the actual value $\varepsilon_p^* = 0.18$ which corresponds to $a_p^* = 0.138\,48$ dB from (29b).

The actual stopband ripple factor will be obtained from (61a)

$$\varepsilon_s^* = \varepsilon_p^* \cdot m_0^2 = 6312.584\,993$$

which gives from (29a) the actual value for $a_s^*$

$$a_s^* = 10\log(1 + 6312.6^2) = 76.00 \text{ dB}.$$

*Determination of the Coefficient Values:*
We compute first the auxiliary parameters given by (62), (63), (64), and (65a). We will have

$$g_1 = \frac{1}{0.18} + \sqrt{\frac{1}{0.18^2} + 1} = 11.200\,393\,69$$
$$g_2 = m_1 g_1 + \sqrt{(m_1 g_1)^2 + 1} = 1.571\,1875 \times 10^6$$
$$g_3 = m_2 g_2 + \sqrt{(m_2 g_2)^2 + 1} = 3.091\,8432 \times 10^{16}$$
$$w_5 = \sqrt[7]{\frac{m_3}{g_3} + \sqrt{\left(\frac{m_3}{g_3}\right)^2 + 1}} = 3.849\,412\,846$$
$$w_4 = \frac{1}{2q_4}\left(w_5 - \frac{1}{w_5}\right) = 4.707\,3 \times 10^{-6}$$

$$w_3 = \frac{1}{2q_3}\left(w_4 - \frac{1}{w_4}\right) = -243.270\,695\,9$$

$$w_2 = \frac{1}{2q_2}\left(w_3 - \frac{1}{w_3}\right) = -8.232\,114\,427$$

$$w_1 = \frac{1}{2q_1}\left(w_2 - \frac{1}{w_2}\right) = -1.488\,597\,056$$

$$w_0 = \frac{1}{2q_0}\left(w_1 - \frac{1}{w_1}\right) = -0.328\,504\,0148.$$

Then the *coefficient value* for $\gamma_0$ from (66a)

$$\gamma_0 = \frac{1 + w_0 q_0 \varphi_p}{1 - w_0 q_0 \varphi_p} = 0.512\,898\,33.$$

In order to calculate the other multiplier values, we compute first the *auxiliary parameters* given by (67), (68), (69), (70a), and (71a).

We will have for $i = 1$

$$c_{4,1} = \frac{381284.9732}{\sin\frac{\pi}{7}} = 8.787\,722\,121 \times 10^5$$

$$c_{3,1} = \frac{1}{2q_3}\left(c_{4,1} + \frac{1}{c_{4,1}}\right) = 1.006\,3209 \times 10^3$$

$$c_{2,1} = \frac{1}{2q_2}\left(c_{3,1} + \frac{1}{c_{3,1}}\right) = 34.053\,820\,41$$

$$c_{1,1} = \frac{1}{2q_1}\left(c_{2,1} + \frac{1}{c_{2,1}}\right) = 6.255\,503\,44$$

$$c_{0,1} = \frac{1}{2q_0}\left(c_{1,1} + \frac{1}{c_{1,1}}\right) = 2.580\,082\,671$$

$$y_1 = \frac{1}{c_{0,1}} = 0.387\,584\,4799$$

$$B_1 = \frac{w_0^2 + y_1^2}{1 + (w_0 y_1)^2}(q_0 \varphi_p)^2 = 0.244\,007\,9871$$

$$A_1 = \frac{-2w_0 q_0 \varphi_p}{1 + (w_0 y_1)^2}\sqrt{1 - \left(q_0^2 + \frac{1}{q_0^2} - y_1^2\right) y_1^2}$$

$$= 0.527\,570\,5195$$

for $i = 2$ in a similar way we have

$$c_{4,2} = \frac{381284.9732}{\sin\frac{2\pi}{7}} = 4.876\,817\,854 \times 10^5$$

$$c_{3,2} = 5.584\,6594 \times 10^2$$

$$c_{2,2} = 18.898\,4865$$

$$c_{1,2} = 3.478\,270\,896$$

$$c_{0,2} = 1.514\,489\,294$$

$$y_2 = \frac{1}{c_{0,2}} = 0.660\,288\,5895$$

$$B_2 = 0.498\,984\,7123$$

$$A_2 = 0.297\,579\,7452$$

and for $i = 3$ we have

$$c_{4,3} = \frac{381284.9732}{\sin\frac{3\pi}{7}} = 3.910\,904\,267 \times 10^5$$

$$c_{3,3} = 4.478\,549\,128 \times 10^2$$

$$c_{2,3} = 15.155\,436\,44$$

$$c_{1,3} = 2.793\,683\,726$$

$$c_{0,3} = 1.267\,500\,656$$

$$y_3 = 0.788\,954\,2267$$

$$B_3 = 0.657\,420\,6341$$

$$A_3 = 0.090\,789\,8113.$$

Then the other coefficient values from (72a) and (73a)

$$\gamma_1 = \frac{A_1 - B_1 - 1}{A_1 + B_1 + 1} = -0.404\,40628$$

$$\gamma_2 = \frac{1 - B_1}{1 + B_1} = 0.607\,70672$$

$$\gamma_3 = \frac{A_2 - B_2 - 1}{A_2 + B_2 + 1} = -0.668\,72355$$

$$\gamma_4 = \frac{1 - B_2}{1 + B_2} = 0.334\,23642$$

$$\gamma_5 = \frac{A_3 - B_3 - 1}{A_3 + B_3 + 1} = -0.896\,134\,00$$

$$\gamma_6 = \frac{1 - B_3}{1 + B_3} = 0.206\,694\,28.$$

In Fig. 13(a)–(d) we can see the block diagram, the signal-flow diagram with optimally scaled structure, the computed attenuation characteristic of this filter and the passband attenuation behavior, respectively.

Additionally, we can compute the *critical frequencies* from (74) and (75). We have

$$f_{\infty,1} = \frac{F}{\pi}\arctan(q_0 \varphi_p / y_1) = 6.082\,08\ \text{kHz}$$

$$f_{\infty,2} = 4.980\,62\ \text{kHz}$$

$$f_{\infty,3} = 4.548\,16\ \text{kHz}$$

and

$$f_{0,1} = \frac{F}{\pi}\arctan(q_0 \varphi_p y_1) = 1.848\,92\ \text{kHz}$$

$$f_{0,2} = 2.925\,23\ \text{kHz}$$

$$f_{0,3} = 3.352\,27\ \text{kHz}.$$

*Example 5*

Cauer parameter (elliptic) bireciprocal low-pass filter

*a) Requirements:*

Stopband: $f_s = 16.3$ kHz $a_s = 65$ dB

Sampling frequency: $F = 64$ kHz.

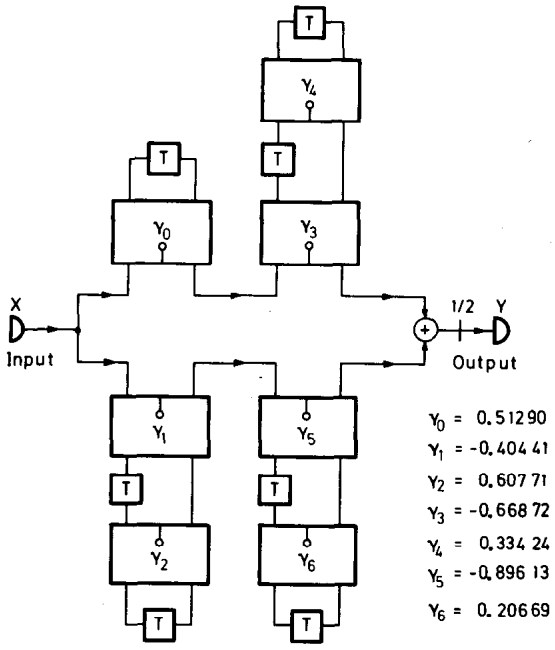


(a)

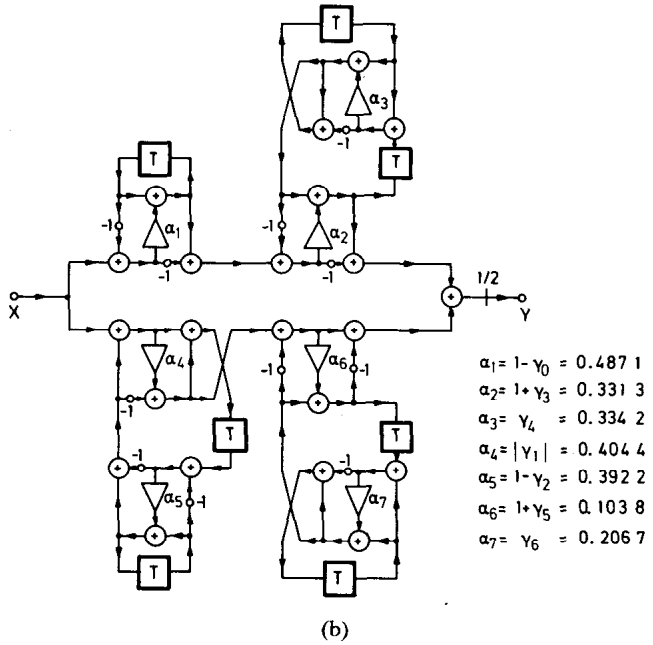


(b)

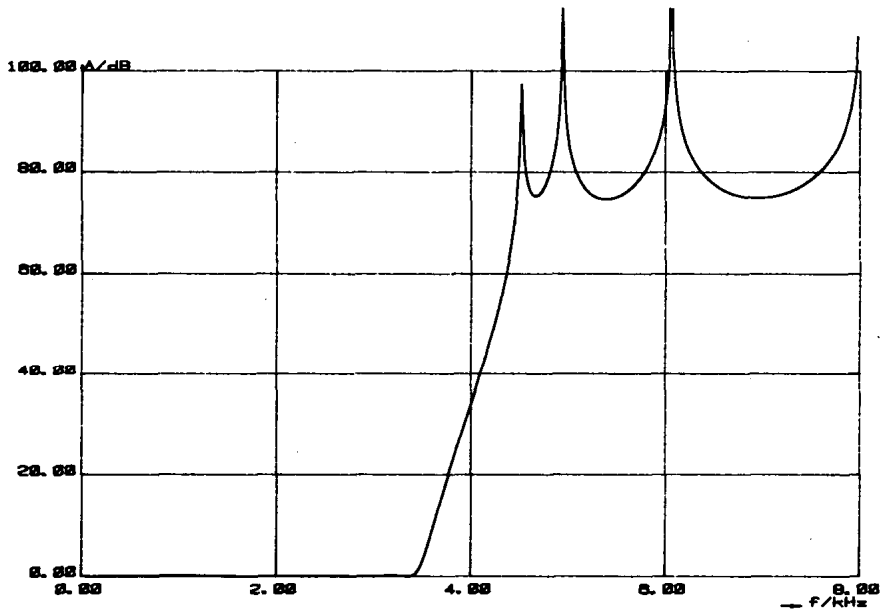


(c)

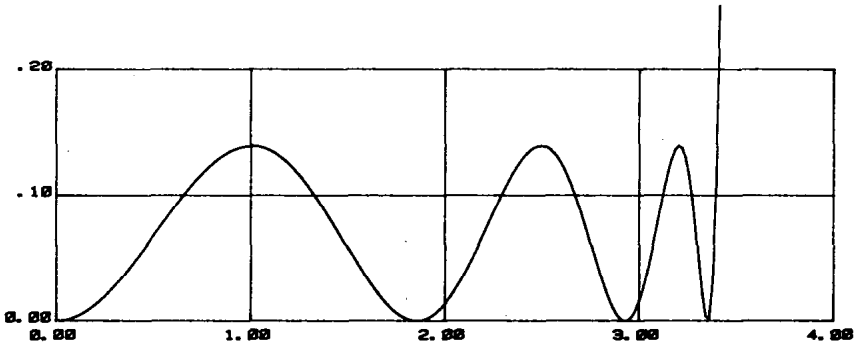


(d)

Fig. 13. Seventh degree WDF with elliptic response. (a) Block diagram. (b) Signal-flow diagram. (c) Attenuation characteristic. (d) Passband behavior.

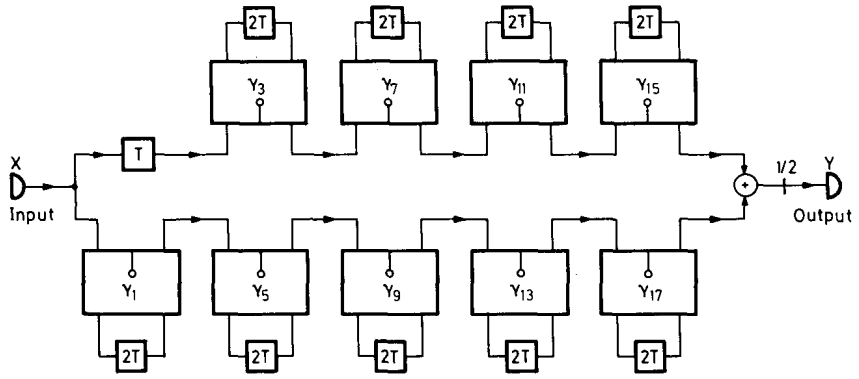


$\gamma_1 = -0.063\,978$ $\gamma_{11} = -0.839\,323$
$\gamma_3 = -0.226\,119$ $\gamma_{13} = -0.905\,567$
$\gamma_5 = -0.423\,068$ $\gamma_{15} = -0.950\,847$
$\gamma_7 = -0.602\,422$ $\gamma_{17} = -0.984\,721$
$\gamma_9 = -0.741\,327$

(a)

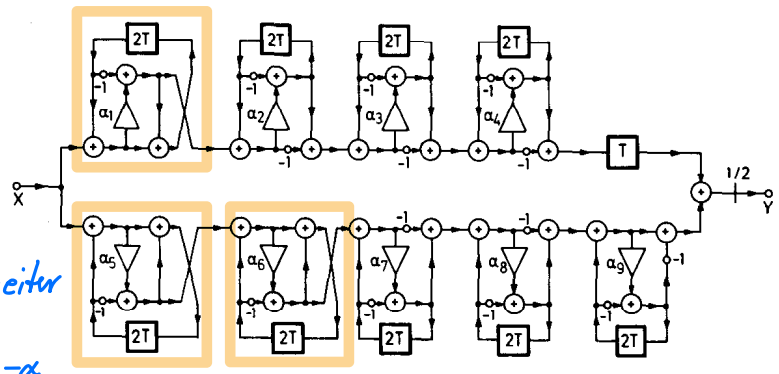


siehe weiter oben:
$\alpha$ soll $-\alpha$ sein bei der Struktur

$\alpha_1 = |\gamma_3| = 0.226\,119$ $\alpha_6 = |\gamma_5| = 0.423\,068$
$\alpha_2 = 1+\gamma_7 = 0.397\,578$ $\alpha_7 = 1+\gamma_9 = 0.258\,673$
$\alpha_3 = 1+\gamma_{11} = 0.160\,677$ $\alpha_8 = 1+\gamma_{13} = 0.094\,433$
$\alpha_4 = 1+\gamma_{15} = 0.049\,153$ $\alpha_9 = 1+\gamma_{17} = 0.015\,279$
$\alpha_5 = |\gamma_1| = 0.063\,978$

(b)

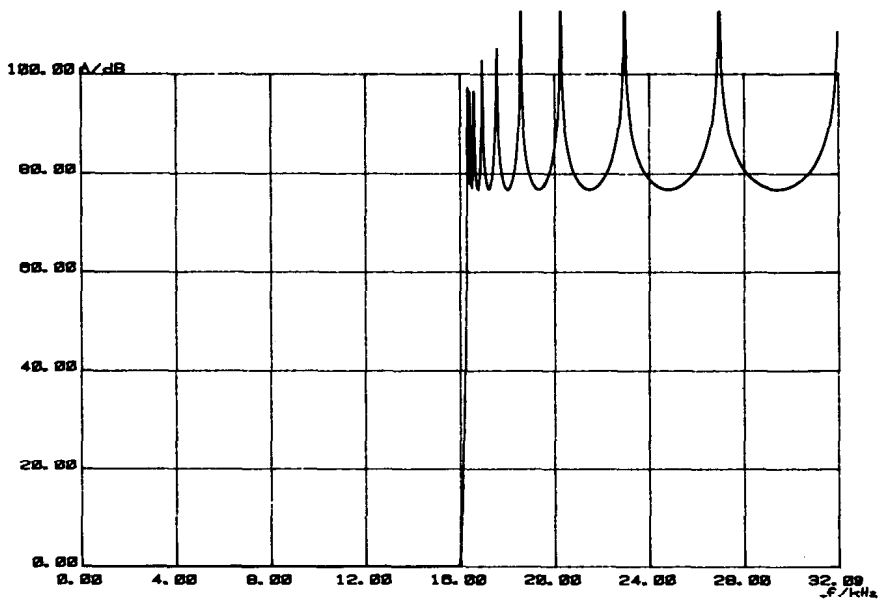


(c)

Fig. 14. Nineteenth degree bireciprocal WDF with elliptic response. (a) Block diagram. (b) Signal-flow diagram. (c) Attenuation characteristic.

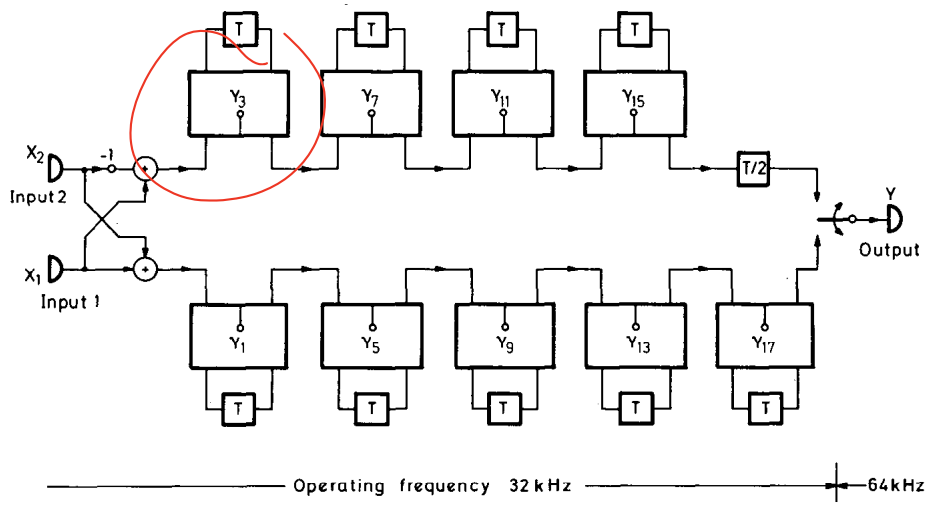


Fig. 15. Nineteenth degree interpolation branching filter derived from the filter given in Fig. 14.

*b) Design procedure:*

Using the restriction (26) and the formulas (27), (28) the design parameters are given by

$$\varepsilon_s = 1778.279\,129$$

$$\varepsilon_p = \frac{1}{\varepsilon_s} = 0.000\,562\,341$$

$$\varphi_s = 1.029\,894\,830$$

$$\varphi_p = \frac{1}{\varphi_s} = 0.970\,972\,929.$$

A *minimum degree* can be estimated by (31) and (32)

$$k_0 = 1.029\,894\,83$$

$$k_1 = 1.414\,306\,312$$

$$k_2 = 3.732\,616\,071$$

$$k_3 = 27.828\,911\,62$$

$$k_4 = 1548.895\,998$$

$$n_{\min} = 16.27.$$

This means we must choose minimum $N=17$, but we will choose $N=19$ because of the larger design margin.

*Determination of the Design Margin:*

Now, we choose $f_s^* = f_s = 16.3$ kHz, i.e., the whole design margin will be given to the stopband (we note that in the actual case the values from (48b), (49)–(51), and (52b) would not be necessary to compute). Since in this case $\varphi_s^* = \varphi_s$ we have that $q_0 = k_0$, $q_1 = k_1$, $q_2 = k_2$, $q_3 = k_3$, and $q_4 = k_4$.

From (57) and (58) we have

$$m_3 = \frac{1}{2}\left(\sqrt{2k_4}\right)^{19} = 7.310\,8254 \times 10^{32}$$

$$m_2 = \sqrt{\frac{1}{2}\left(m_3 + \frac{1}{m_3}\right)} = 1.911\,9134 \times 10^{16}$$

$$m_1 = \sqrt{\frac{1}{2}\left(m_2 + \frac{1}{m_2}\right)} = 97773037.2$$

$$m_0 = \sqrt{\frac{1}{2}\left(m_1 + \frac{1}{m_1}\right)} = 6991.889\,487.$$

Then, from (59b) we have the minimum value of the passband ripple factor

$$\varepsilon_{p\,\min} = \frac{1}{m_0} = 1.430\,228\,555 \times 10^{-4}.$$

We choose $\varepsilon_p^* = \varepsilon_{p\,\min}$, i.e., the whole design margin will be given to the stopband and in the same manner to the passband according to the bireciprocal property (see (26)). From (61b) we have

$$\varepsilon_s^* = m_0 = 6991.889\,487$$

which corresponds to a loss value from (29a)

$$a_{s\,\max}^* = 10\log\left(1 + m_0^2\right) = 76.89\,\text{dB}.$$

*Determination of the Coefficient Values:*

In the bireciprocal case we need compute only the auxiliary parameters given by (67)–(69) and (71b). We will have for $i=1$

$$c_{4,1} = \frac{1548.895998}{\sin\frac{\pi}{19}} = 9410.370\,02$$

$$c_{3,1} = \frac{1}{2k_3}\left(c_{4,1} + \frac{1}{c_{4,1}}\right) = 169.075\,425$$

$$c_{2,1} = \frac{1}{2k_2}\left(c_{3,1} + \frac{1}{c_{3,1}}\right) = 22.649\,173\,7$$

$$c_{1,1} = \frac{1}{2k_1}\left(c_{2,1} + \frac{1}{c_{2,1}}\right) = 8.022\,775\,99$$

$$c_{0,1} = \frac{1}{2k_0}\left(c_{1,1} + \frac{1}{c_{1,1}}\right) = 3.955\,462\,678$$

$$y_1 = \frac{1}{c_{0,1}} = 0.252\,814\,9249$$

$$A_1 = \frac{2}{1+y_1^2}\sqrt{1 - \left(k_0^2 + \frac{1}{k_0^2} - y_1^2\right)y_1^2}$$

$$= 1.759\,474\,658.$$

Then from (72b)

$$\gamma_1 = \frac{A_1 - 2}{A_1 + 2} = -0.063\,978.$$

In a similar way we obtain for $i = 2$ until 9

$$\gamma_3 = -0.226\,119$$
$$\gamma_5 = -0.423\,068$$
$$\gamma_7 = -0.602\,422$$
$$\gamma_9 = -0.741\,327$$
$$\gamma_{11} = -0.839\,323$$
$$\gamma_{13} = -0.905\,567$$
$$\gamma_{15} = -0.950\,847$$
$$\gamma_{17} = -0.984\,721.$$

In Fig. 14(a)–(c) we can see the block diagram, the signal-flow diagram with optimally scaled structure and the computed attenuation characteristic of this filter, respectively.

We note that sampling rate alteration by factor two can be very economically combined with this filter. In Fig. 15 we can see an interpolation branching filter based on the above design. We can observe that both lattice branches operate on the lower sampling rate (32 kHz) and the output sequence is obtained by interleaving the output sequences of the lattice branches. We mention finally that this type of filters can be properly used in certain transmultiplexer applications [10], [51].

## ACKNOWLEDGMENT

The author is very grateful to Dr. A. Fettweis for the valuable discussions on the subject of this paper and to S. N. Güllüoglu for his help in controlling work.

## REFERENCES

[1] A. Fettweis, "Digital filter structures related to classical networks", *Arch. Elek. übertragung.*, vol. 25, pp. 79–89, Feb. 1971.
[2] ____, "Digital circuit and systems," vol. CAS-31, pp. 31–48, Jan. 1984.
[3] A. Fettweis, H. Levin, and A. Sedlmeyer, "Wave digital lattice filters," *Int. J. Circuit Theory Appl.*, vol. 2, no. 2, pp. 203–211, June 1974.
[4] R. Nouta, "The use of Jaumann structures in wave digital filters," *Int. J. Circuit Theory Appl.*, vol. 2, pp. 163–174, June 1974.
[5] W. Wegener, "On the design of wave digital lattice filters with short coefficient word lengths and optimal dynamic range," *IEEE Trans. Circuits Syst.*, vol. CAS-25, pp. 1091–1098, Dec. 1978.
[6] W. Wegener, "Entwurf von Wellendigitalfiltern mit minimalem Realisierungsaufwand," Doctoral dissertation, Ruhr-Universität Bochum, Bochum, West Germany, 1980.
[7] W. Wegener, "Wave digital directional filters with reduced number of multipliers and adders," *Arch. Elek. übertragung.*, vol. 33, no. 6, pp. 239–243, June 1979.
[8] A. Fettweis, "Transmultiplexers with either analog conversion circuits, wave digital filters, or SC-filters—A review," *IEEE Trans. Commun.*, vol. COM-30, pp. 1575–1586, July 1982.
[9] L. Gazsi, "Single chip filter bank with wave digital filters," *IEEE Trans. Acoust., Speech, Signal Processing*, vol. ASSP-30, pp. 709–718, Oct. 1982.
[10] J. A. Nossek and H. -D. Schwartz, "Wave digital lattice filters with application in communication systems," Proc. 1983 IEEE Int. Symp. Circuits and Systems, pp. 845-848, Newport Beach, CA, May 1983.
[11] S. Darlington, "Analytical approximations to approximations in the Chebyshev sense," *Bell Syst. Tech. J.*, vol. 49, no. 1, pp. 1–32, Jan. 1970.
[12] ____, "Simple algorithms for elliptic filters and generalizations thereof," *IEEE Trans. Circuits Syst.*, vol. CAS-25, pp. 975–980, Dec. 1978.
[13] V. Belevitch, Classical Network Theory. San Francisco, CA: Holden Day, 1968.
[14] A. Fettweis, "Cascade synthesis of lossless two-ports by transfer matrix fractorization," in *Proc. 1969 NATO Advanced Study Institute on Network Theory*, (ed. R. Boite), Gordon and Breach, NY, 1972.
[15] J. D. Rhodes, "Theory of electrical filters," London: Wiley, 1976.
[16] A. Antoniou, *Digital Filters: Analysis and Design*. New York: McGraw-Hill, 1979.
[17] G. Bosse and W. Nonnenmacher, "Einheitliche Formeln für Filter mit Tschebyscheff-Verhalten der Betriebsdämpfung," *Frequenz*, vol. 13, pp. 33–44, Feb. 1959.
[18] J. K. Skwirzynski, "Design theory and data for electrical filters," London: Van Nostrand, 1965.
[19] E. Christian and E. Eisenmann, Filter design tables and graphs. New York: Wiley, 1966.
[20] A. I. Zverev, *Handbook of Filter Synthesis*. New York: Wiley, 1967.
[21] R. Saal, "Handbook of filter design," Backnang, Germany, AEG-Telefunken, 1979.
[22] A. H. Gray Jr., J. D. Markel, "A computer program for designing digital elliptic filters," *IEEE Trans. Acous., Speech, Signal Processing*, vol. ASSP-24, pp. 529–538, Dec. 1976.
[23] P. Amstutz, "Elliptic approximation and elliptic filter design on small computers," *IEEE Trans. Circuits Syst.*, vol. CAS-25, pp. 1001–1011, Dec. 1978.
[24] Digital Signal Processing Committee, "Programs for digital signal processing," IEEE Press., New York: Wiley, 1979.
[25] E. Avenhaus, H. W. Schüssler, "On the approximation problem in the design of digital filters with limited wordlength," *Arch. Elek. übertragung.*, vol. 24, no. 12, pp. 571–572, Dec. 1970.
[26] K. -A. Owenier, "Optimierung von Filtern, insbesondere von Wellendigitalfiltern mit verringerter Zahl an Multiplizierern", Ph.D. dissertation, Ruhr-Universität Bochum, West Germany, July 1977.
[27] ____, "Optimization of wave digital filters with reduced number of multipliers," *Arch. Elek. übertragung.*, vol. 30, No. 10, pp. 378–393, Oct., 1976.
[28] K. Steiglitz, "Designing short-word recursive digital filters," in *Proc. ninth ann. Allerton Conf. Circuit and Syst. Theory*, pp. 778–785, Oct., 1971, also in *Digital Signal Processing II*, IEEE Press, NY, 1975.
[29] F. Brglez, "Digital filter design with short word-length coefficients," *IEEE Trans. Circuits Syst.*, vol. CAS-25, pp. 1044–1050, Dec. 1978.
[30] L. Gazsi, S. N. Güllüoglu, "Discrete optimization of coefficients in CSD code," *Proc. Mediterranean Electrotechnical Conf.*, (Athens, Greece), pp. C03.08-9, May 1983.
[31] A. Fettweis, private communication 1980.
[32] L. Weinberg, *Network Analysis and Synthesis*. New York: McGraw-Hill, 1962.
[33] L. Gazsi, "Optimal scaling of lattice wave digital filters for sinusoidal excitation," to be published.
[34] A. Fettweis and K. Meerkötter, "On adaptors for wave digital filters," *IEEE Trans. Acoust., Speech, Signal Processing*, vol. ASSP-23, pp. 516–525, Dec. 1975.
[35] L. B. Jackson, "On the interaction of roundoff noise and dynamic range in digital filters," *Bell Syst. Tech. J.*, vol. 49, pp. 159–184, Feb. 1970.
[36] A. Fettweis, K. Meerkötter, "Supression of parasitic oscillations in wave digital filters," *IEEE Trans. Circuits Syst.*, vol. CAS-22, pp. 239–246, Mar. 1975 and p. 575, June 1975.
[37] L. Gazsi, "Hardware implementation of wave digital filters using programmable digital signal processors," *Proc. European Conf. Circuit Theory and Design* (ECCTD-81), pp. 1052–1057, (The Hague, The Netherlands), Aug. 1981.
[38] K. Meerkötter, "Beiträge zur Theorie der Wellendigital-filter," doctoral dissertation, Ruhr-Universität Bochum, Bochum, West Germany, 1979.
[39] K. Meerkötter, "Incremental pseudopassivity of wave digital filters," *Proc. First European Signal Processing Conf.* (EUROSIP-80), pp. 27–32, (Lausanne, Switzerland), Sept. 1980.
[40] T. A. C. M. Claasen, W. F. G. Mecklenbräuker, and J. B. H. Peek, "On the stability of the forced respose of digital filters with overflow nonlinearities," *IEEE Trans. Circuits Syst.*, vol. CAS-22, pp. 692–696, Aug. 1975.
[41] A. Fettweis and K. Meerkötter, "On parasitic oscillations in digital filters under looped conditions," *IEEE Trans. Circuits Syst.*, vol. CAS-24, pp. 475–481, Sept. 1977.
[42] L. Wanhammar, "An approach to LSI implementation of wave digital filters," doctoral dissertation, (Linköping University, Sweden), 1981.
[43] A. H. Gray and J. D. Markel, "Digital lattice and ladder filter synthesis", *IEEE Trans. Audio and Electroacoust.*, vol. AU-21, pp. 491–500, Dec. 1973.
[44] J. D. Markel and A. H. Gray, Jr., *Linear Prediction of Speech*. Berlin, W. Germany: Springer-Verlag, 1976.
[45] A. H. Gray, Jr., "Passive cascaded lattice digital filters," IEEE Trans. Circuits Syst., vol. CAS-27, pp. 337–344, May 1980.
[46] P. B. Denyer, D. Renshaw, and N. Bergmann, "A silicon compiler for VLSI signal processors," in *Proc. Europ. Conf. Solid State Circuits*, pp. 215–218, (Brussels, Belgium), Sept., 1982.
[47] H. M. Reekie, J. Mavor, N. Petrie, and P. B. Denyer, "An automated design procedure for frequency selective wave filters," in *Proc. IEEE Int. Symp. Circuits Syst.*, vol. 1, pp. 258–261, (Newport Beach, CA), May 1983.
[48] H. De Man, J. Van Ginderdeuren, F. Catthoor, and S. Bechers, "Study of the realization of wave digital filters on custom integrated circuits," Internal Report ESAT, Okt. 1982.
[49] O. E. Herrmann and J. Smit, "A user-friendly environment to

implement algorithms on single-chip digital signal processors," in *Proc. Second European Signal Proc. Conf.*, EUROSIP '83, pp. 851–854, (Erlangen, W. Germany), Sept. 1983.
[50] R. H. Cushman, "Signal-processing design awaits digital take-over," EDN Mag., pp. 119–128, June 24, 1981.
[51] L. Gazsi, "Single-path transmultiplexer scheme with multirate wave digital filters," in *Proc. IEEE Int. Conf. Communications* (ICC '84), pp. 675–678, (Amsterdam), May 1984.

✤

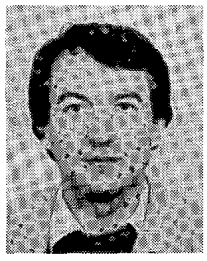

**Lajos Gazsi** (M'83–SM'84) was born in Kaposvár, Hungary, on February 17, 1942. He received the Diploma and the Doctor Techn. degree in electrical engineering from the Technical University of Budapest, Hungary, in 1964 and 1974, respectively, and the Candidate of Technical Sciences degree in circuit theory from the Hungarian Academy of Sciences, Budapest, in 1974.

He worked in the Department of Measurement and Instrument, Technical University of Budapest, Hungary, from 1964. In 1974, he spent a year on leave, with A. Fettweis in the Department of Electrical Engineering, Ruhr-University Bochum, West Germany. He has been employed there since 1977, working mainly in the field of digital signal processing. In addition to the theoretical work he has been taking part in the design of a sophisticated digital signal processor that is being developed at Siemens Company in Munich, West Germany, in 1983. Furthermore, he is participating in the ESPRIT project "European Strategic Programme for Research and Development in Information Technology" sponsored by the European Community. The prime contractor is Professor H. DeMan from the ESAT Laboratory, Katholieke Universiteit, Leuven, Belgium.

Dr. Gazsi is a member of the European Association for Signal Processing (EURASIP).

# Transactions Briefs

## On Error-Spectrum Shaping in State-Space Digital Filters

P. P. VAIDYANATHAN

*Abstract*—**A new scheme for shaping the error spectrum in state-space digital filter structures is proposed. The scheme is based on the application of diagonal second-order error feedback, and can be used in any arbitrary state-space structure having arbitrary order. A method to obtain noise-optimal state-space structures for fixed error feedback coefficients, starting from noise optimal structures in absence of error feedback (the Mullis and Roberts Structures), is also outlined. This optimization is based on the theory of continuous equivalence for state-space structures.**

### I. Introduction

The use of error spectrum shaping (ESS) for roundoff noise reduction in (narrow band) recursive digital filters is well known, and a number of interesting research contributions in this area have appeared [1]–[5] in the last few years. The application of this idea to state-space structures is mentioned in [2], and some studies in this connection have already been reported in [5]. In [7], Mullis and Roberts clarify the relation between error feedback (EFB) techniques and double precision implementations in state-space structures, among others.

The purpose of this paper is to outline a new procedure for choice of EFB coefficients in state-space structures. Specifically, we extend the feedback scheme proposed in [2] and [5] by incorporating an additional higher order matrix term. We do not consider error feedforward in this paper. We choose the EFB coefficients such that each noise source is "shaped" independent of others. In the resulting structures, each noise source is essentially replaced by an equivalent source which is no more white, but has zeros on the unit circle of the $z$-plane, at suitable locations. Consequently the major portion of noise power moves into the stopband. The overall noise is thus reduced, by the time it reaches the filter output. (It should be noticed that the idea of introducing zeros into the noise spectrum is itself not new, and is indeed the basis in [1].)

In such a structure, we essentially have "colored" noise sources, and the optimal state space structure for a given noise-spectral shaping is in general different from that for white noise sources. Based on the fundamental results on minimum-noise state-space structures [6] for uncorrelated white noise sources, we outline an iterative procedure for arriving at the minimum-noise structure with fixed EFB. The procedure is based on applying a sequence of similarity transformations in such a way that at each iteration there is an improvement in the objective function.

In Section II we deal with the shaping of error spectrum for a given state-space structure. In Section III, we outline the state-space optimization for a given ESS shaping.

### II. Noise Shaping

Consider the standard state-space representation:

$$x(n+1) = \boldsymbol{A}x(n) + \boldsymbol{B}u(n) \tag{1a}$$

$$y(n) = \boldsymbol{C}x(n) + \boldsymbol{D}u(n). \tag{1b}$$

Here $\boldsymbol{A}$ is an $N \times N$ matrix, $\boldsymbol{B}$ is $N \times 1$, $\boldsymbol{C}$ is $1 \times N$, and $\boldsymbol{D}$ is $1 \times 1$. We assume that the only quantization involved is in the implementation of $\boldsymbol{A}x(n)$, as this is the only error that propagates through the feedback path. Fig. 1 shows the conventional EFB scheme, where the error vector due to the vector quantizer is fedback through a delay (to avoid delay free loops). The matrix

Manuscript received September 13, 1983; revised March 1, 1984. This work was supported in part by the National Science Foundation under Grant ECS82-18310 and in part by Caltech funds.

The author is with the Department of Electrical Engineering, California Institute of Technology, Pasadena, CA 91125.

0098-4094/85/0100-0088$01.00 ©1985 IEEE